Published December 1, 1996

MHP1, an Essential Gene in *Saccharomyces cerevisiae* Required for Microtubule Function

Irmgard Irminger-Finger,* Ed Hurt,§ Aline Roebuck,* Martine A. Collart‡, and Stuart J. Edelstein*

*Department of Biochemistry, ‡Department of Medical Biochemistry, University of Geneva, 1211 Geneva 4, Switzerland; and §EMBL, 69012 Heidelberg, Germany

Abstract. The gene for a microtubule-associated protein (MAP), termed *MHP1* (MAP-Homologous Protein 1), was isolated from *Saccharomyces cerevisiae* by expression cloning using antibodies specific for the *Drosophila* 205K MAP. *MHP1* encodes an essential protein of 1,398 amino acids that contains near its COOH-terminal end a sequence homologous to the microtubule-binding domain of MAP2, MAP4, and tau. While total disruptions are lethal, NH_2-terminal deletion mutations of *MHP1* are viable, and the expression of the COOH-terminal two-thirds of the protein is sufficient for vegetative growth. Nonviable deletion–disruption mutations of *MHP1* can be partially complemented by the expression of the *Drosophila* 205K MAP. Mhp1p binds to microtubules in vitro, and it is the COOH-terminal region containing the tau-homologous motif that mediates microtubule binding. Antibodies directed against a COOH-terminal peptide of Mhp1p decorate cytoplasmic microtubules and mitotic spindles as revealed by immunofluorescence microscopy. The overexpression of an NH_2-terminal deletion mutation of *MHP1* results in an accumulation of large-budded cells with short spindles and disturbed nuclear migration. In asynchronously growing cells that overexpress *MHP1* from a multicopy plasmid, the length and number of cytoplasmic microtubules is increased and the proportion of mitotic cells is decreased, while haploid cells in which the expression of *MHP1* has been silenced exhibit few microtubules. These results suggest that *MHP1* is essential for the formation and/or stabilization of microtubules.

MICROTUBULES (MTs)[1] are involved in a number of essential cellular processes such as cell morphogenesis, intracellular transport, cell motility, and mitosis. Important potential regulators of MT dynamics are the MT-associated proteins (MAPs) (Lee, 1993; Wiche et al., 1991). Initially MAPs were isolated from neural tissues rich in MTs by means of copurification with polymerized MTs. These neural MAPs, including MAP 1A (Schoenfeld et al., 1989), MAP 1B (Noble et al., 1989), MAP2 (Lewis et al., 1988), and tau (Lee et al., 1988), were shown to stimulate MT assembly from purified tubulin in vitro (Cleveland et al., 1977; Murphy et al., 1977; Bulinski and Borisy, 1979). Although these MAPs have been characterized biochemically, their specific functions have not been determined unambiguously.

A group of ubiquitously expressed, thermostable MAPs has also been described as phosphorylated proteins of ~200 kD (MAP4-type proteins) comprising (as in the case of MAP1, MAP2, and tau) multiple protein isoforms. Immunocytochemistry has shown that these MAPs colocalize with mitotic spindle and interphase MTs (Bulinski and Borisy, 1980; Izant et al., 1983). Cloning and sequencing of mouse, human (Chapin and Bulinski, 1991; West et al., 1991), and bovine (Aizawa et al., 1990) MAP4 have revealed that the MAP4 proteins share an MT-binding domain homologous to the MT-binding motif first discovered in tau and MAP2 (Lee et al., 1988; Lewis et al., 1988). The common sequence motif, the assembly promoting (AP) sequence (Aizawa et al., 1989), consists of three or four basic repeats of 31 amino acid residues within the COOH-terminal domain of the proteins.

In several species MAPs of ~200 kD have been discovered that are immunologically related to the *Drosophila* 205K MAP but not to MAP4-type proteins (Kimble et al., 1992). The *Drosophila* 205K MAP was analyzed and found to contain no sequence homologies to other MAPs. Moreover, it possesses an MT-binding region without homology to tau, MAP2, or MAP4 (Irminger-Finger et al., 1990). However, the 205K MAP is similar to MAP4 and MAP2 in terms of an extensive NH_2-terminal acidic region

Address all correspondence to Stuart J. Edelstein, Department of Biochemistry, University of Geneva, 30 quai Ernest-Ansermet, 1211 Geneva 4, Switzerland. Tel.: (41) 22 702 64 86. Fax: (41) 22 702 64 76. e-mail: Stuart.Edelstein@biochem.unige.ch

1. *Abbreviations used in this paper*: ADH, alcohol dehydrogenase; AP, assembly promoting; DAPI, 4′,6-diamidino-2-phenylindole; MAP, microtuble-associated protein; MT, microtubule; NLS, nuclear localization signal; ORF, open reading frame; SPB, spindle pole body.

Published December 1, 1996

and, as in the case of tau, a short, acidic COOH-terminal region that is preceded by a basic region containing the MT-binding domain.

The in vivo functions of all the MAPs identified so far remain uncertain, mainly because of the absence of genetic studies. In the isolated case of the *Drosophila* 205K MAP where such studies were possible, the protein was found not to be essential (Pereira et al., 1992). A powerful tool to more fully investigate the functions of MAPs is the yeast *Saccharomyces cerevisiae*, since it is possible to establish genetic interactions between MAPs and tubulin or other cytoskeletal components. A number of laboratories have attempted to identify MAPs in yeast. Their approaches have involved purifying proteins by MT-affinity columns (Barnes et al., 1992) or from cellular structures comprising MTs such as the spindle pole body (SPB) (Kilmartin et al., 1993) and the centromere-binding complex (Jiang et al., 1993), identifying yeast proteins that cross-react with antibodies against mammalian MAPs (Hasek et al., 1991), cloning genes complementing cellular defects involving MTs (Hoyt et al., 1990; Stearns et al., 1990; McMillan and Tatchell, 1994), and cloning yeast sequences using PCR with degenerated primers derived from homologous sequences of different species (Hyman et al., 1992). These strategies led to the identification of CPF5p, a component of the yeast centromere-binding complex, a homologue of mammalian MAP1A and B (Jiang et al., 1993), and a number of genes encoding proteins that share similarities with motor proteins (Berlin et al., 1990; Meluh and Rose, 1990; Hoyt et al., 1992; Lillie and Brown, 1992; Roof et al., 1992; Li et al., 1993). In a biochemical approach, Sep1 has been identified as an accessory protein in MT function in yeast (Interthal et al., 1995). A genetic screen for complementation of a temperature-sensitive allele of the β-tubulin gene led to the identification of *STU1*, a gene encoding a protein with a predicted size of 174 kD and no significant homology to known proteins (Pasqualone and Huffaker, 1994).

We chose to search for yeast proteins that cross-react with antibodies directed against the *Drosophila* 205K MAP, leading to the discovery of a novel essential MAP gene, *MHP1* (MAP Homologous Protein 1). We present evidence that the product of this gene, Mhp1p, interacts with MTs and that mutations in *MHP1* influence MT structure and function during interphase and mitosis.

Materials and Methods

Strains and Microbiological Techniques

All yeast strains used in this study are listed in Table I. Genetic manipulations and growth media were standard (Sherman et al., 1986; Rose et al., 1990).

Cloning of MHP1

A partial sequence of the *MHP1* gene was cloned by screening a λgt11 cDNA expression library from *S. cerevisiae* (kindly provided by Dr. B. Altman, University of Bern, Switzerland). 20,000 plaques were screened and plated in Y1090r$^-$ host cells to a plaque density of 1,000–2,000 plaques per plate. Plates were incubated at 42°C for 4 h, or until very small plaques were visible, then overlaid with nitrocellulose filters previously soaked in 10 mM isopropyl β-D-thiogalactopyranoside (IPTG), and incubated for 4 h at 37°C. Filters were blocked with 3% BSA in TBS for 30 min, washed with TBS, and incubated with a polyclonal anti-205K MAP antibody (Goldstein et al., 1986) in a 1:500 dilution for 2 h at room temperature. After washing with TBS, the secondary antibody, a mouse anti–IgG coupled to alkaline phosphatase (Sigma Chemical Co., St. Louis, MO), was applied in a 1:5,000 dilution. Positive phages were visualized with 5-bromo-4-chloro-3-indolylphosphate disodium salt (BCIP) and nitro blue tetrazolium (NBT) (Sigma Chemical Co.). Plaques in the region of the signal were resuspended in phage buffer (10 mM Tris, pH 7.5, 10 mM $MgCl_2$), replated, and rescreened with the same procedures. Three positive plaques were obtained and tested for the expression of the immunoreactive protein on Western blots. The insert of one phage was subcloned into the Bluescript-vector (pBS) and sequenced, the 740-bp insert was used as radioactive probe to screen a library of genomic DNA partially digested by Sau3A (kindly provided by Dr. B. Dujon, Institute Pasteur, Paris, France), and the clone F2B8 was isolated and sequenced. General molecular cloning techniques were as described (Maniatis et al., 1989).

DNA Sequence Analysis

DNA sequencing was performed with the dideoxy chain termination method (Sanger et al., 1977), using the Sequenase kit (UBS; United States Biochemical Corp., Cleveland, OH). Both strands of the genomic region containing the *MHP1* gene were sequenced on average twice. Sequence data were assembled and analyzed with the Genetics Computer Group programs (Devereux et al., 1984).

Computer Analysis of the MHP1 Sequence

Secondary structure analysis of the amino acid sequence of *MHP1* was performed using the algorithms of Garnier et al. (1978) and Chou and Fasman (1978). The protein databases PIR and Swissprot were searched with the entire Mhp1p sequence using FASTA (Pearson and Lipman, 1988). The sequence of Mhp1p was compared directly to sequences of known MAPs using FASTA and PILEUP (Devereux et al., 1984).

In Vitro Transcription–Translation

Coupled in vitro transcription and translation were performed with a transcription–translation kit (Promega Corp., Madison, WI) and [^{35}S]methionine, according to the manufacturer's instructions. For each reaction 2 μg of plasmid DNA were used. N1300 was a subclone in pBS containing the region from bp 656–3,662, and N1121 was generated by restriction digestion. Construct C1188 was generated by subcloning the PCR-amplified region from bp 3,562–4,368 into pBS.

MT-binding Assay

MT-binding assays were performed using porcine brain tubulin, purified by phosphocellulose chromatography. MTs were preassembled and stabilized in the presence of 2 mM GTP and 20 μm taxol as described (Vallee, 1982). To test the MT-binding activity of the in vitro–translated proteins, the reaction mixture was centrifuged to precipitate nonsoluble material, protease inhibitors were added to the assembly reaction, and 4 μl of the in vitro translation reactions was added to assembled MTs in a total volume of 25 μl. When Mhp1p from yeast cells was tested, protease inhibitors were added to the assembly reaction before addition of 15 μl total yeast protein extract in a total of 50 μl. Yeast cells (100 μg) were lysed in 100 μl lysis buffer (100 mM Pipes-KOH, pH 6.9, 2 mM EGTA, 1 mM $MgCl_2$) by vigorous vortexing (30 s) with glass beads and immediately used for the binding assay to minimize the degradation of Mhp1p. Assembly reactions were centrifuged, pellets were rinsed with assembly buffer and recentrifuged, and supernatants and pellets were analyzed by PAGE.

Antibody Production and Purification

The COOH-terminal region of *MHP1* from bp 3,562–4,368 was amplified by PCR, generating terminal NdeI sites, and cloned into the NdeI site of the His-tag expression vector pET-15b (Studier et al., 1990), generating the plasmid pET-C1188, which was expressed in *Escherichia coli*. The apparent molecular mass of the His-tagged protein expressed by pET-C1188 was 36-kD on SDS gels. The 36-kD protein, termed C1188p, was purified on "His-bind" resin (Novagen, Madison, WI), and 100 μg was injected subcutaneously into rabbits. The collected sera were centrifuged, and the supernatant was immunopurified on membrane-bound antigen as described (Olmsted, 1986).

Published December 1, 1996

Table I. Saccharomyces cerevisiae Strains Used in This Study

Name		Genotype	Sources
Y501	2n	*a/α ura3-52 lys2-801$_a$ ade2-101$_0$ trp1-Δ63 his3-Δ200 leu2-Δ1*	P. Hieter
Y502	2n	*a/α ura3-52 lys2-801$_a$ ade2-101$_0$ trp1-Δ63 his3-Δ200 leu2-Δ1 mhp1$^+$/mhp1-Δ1::TRP1*	This work
Y503	2n	*a/α ura3-52 lys2-801$_a$ ade2-101$_0$ trp1-Δ63 his3-Δ200 leu2-Δ1 mhp1$^+$/mhp1-Δ1::TRP1* [pADN-205]	This work
Y504	n	*a/α ura3-52 lys2-801$_a$ ade2-101$_0$ trp1-Δ63 his3-Δ200 leu2-Δ1 mhp1-Δ1::TRP1* [pADN-205]	This work
Y505	2n	*a/α ura3-52 lys2-801$_a$ ade2-101$_0$ trp1-Δ63 his3-Δ200 leu2-Δ1* [pMAC-Pst]	This work
Y506	2n	*a/α ura3-52 lys2-801$_a$ ade2-101$_0$ trp1-Δ63 his3-Δ200 leu2-Δ1 mhp1$^+$/mhp1-Δ1::TRP1* [pMAC-Pst]	This work
Y507	2n	*a/α ura3-52 lys2-801$_a$ ade2-101$_0$ trp1-Δ63 his3-Δ200 leu2-Δ1* [pMACmyc-Pst]	This work
Y508	2n	*a/α ura3-52 lys2-801$_a$ ade2-101$_0$ trp1-Δ63 his3-Δ200 leu2-Δ1* [pMAC-Bam]	This work
Y509	2n	*a/α ura3-52 lys2-801$_a$ ade2-101$_0$ trp1-Δ63 his3-Δ200 leu2-Δ1* [Yep-MPH]	This work
Y521	2n	*a/α ura3-52 lys2-801$_a$ ade2-101$_0$ trp1-Δ63 his3-Δ200 leu2-Δ1 mhp1$^+$/mhp1-Δ4::TRP1*	This work
Y531	2n	*a/α ura3-52 lys2-801$_a$ ade2-101$_0$ trp1-Δ63 his3-Δ200 leu2-Δ1 mhp1$^+$/mhp1-Δ5::HIS3*	This work
Y105	2n	*a/α ura3-52 lys2-801$_a$ ade2-101$_0$ trp1-Δ63 his3-Δ200 leu2-Δ1 mhp1$^+$/mhp1-Δ2::URA3*	This work
Y106	n	*α ura3-52 lys2-801$_a$ ade2-101$_0$ trp1-Δ63 his3-Δ200 leu2-Δ1 mhp1-Δ2::URA3*	This work
Y561	2n	*a/α ura3-52 lys2-801$_a$ ade2-101$_0$ trp1-Δ63 his3-Δ200 leu2-Δ1 mhp1$^+$/mhp1-Δ6::kan^r*	This work
Y562	2n	*a/α ura3-52 lys2-801$_a$ ade2-101$_0$ trp1-Δ63 his3-Δ200 leu2-Δ1 mhp1$^+$/mhp1-Δ6::kan^r* [pMAC-MHP]	This work
Y563	2n	*a/α ura3-52 lys2-801$_a$ ade2-101$_0$ trp1-Δ63 his3-Δ200 leu2-Δ1 mhp1$^+$/mhp1-Δ6::kan^r* [pMAC-Pst]	This work
Y564	n	*α ura3-52 lys2-801$_a$ ade2-101$_0$ trp1-Δ63 his 3-Δ200 leu2-Δ1 mhp1-Δ6::kan^r* [pMAC-MHP]	This work
Y565	2n	*a/α ura3-52 lys2-801$_a$ ade2-101$_0$ trp1-Δ63 his3-Δ200 leu2-Δ1 mhp1$^+$/mhp1-Δ6::kan^r* [pADN-205]	This work
Y566	n	*α ura 3-52 lys2-801$_a$ ade2-101$_0$ trp1-Δ63 his3-Δ200 leu2-Δ1 mhp1-Δ6::kan^r* [pADN-205]	This work

Tubulin-binding Assay

Crude bacterial lysates from 200 ml cultures of *E. coli* expressing C1188p from plasmid pET-C1188 or the His-tagged NH_2-terminal region of *MHP1*, encoding amino acids 1–440, from plasmid pET-N440, were loaded onto His-bind resin columns. PET-N440 had been generated by cloning the PCR-amplified coding region of *MHP1* with terminal NdeI sites into the NdeI site of pET-15. Deletion of the 3′ XhoI fragment and religation allowed the creation of pET-N440. The Ni-columns were washed with standard His-bind binding buffer, equilibrated with 100 mM Pipes, pH 6.9, and loaded with a crude protein extract from 1 g of frozen *S. cerevisiae* strain Y501 prepared in 4 ml MT-binding buffer. Columns were washed extensively with Pipes and eluted with His-bind elution buffer. Column fractions were analyzed by PAGE and Western blotting.

Western Blots

Blotting procedures were performed as described (Ortega Perez et al., 1994). The membranes were incubated at room temperature for 2 h with anti-MHP1 in a 1:200 dilution, or anti-205K MAP in a 1:500 dilution. The secondary antibody was alkaline phosphatase–conjugated anti–rabbit IgG (Sigma Chemical Co.), in a 1:5,000 dilution, and the reaction was visualized by BCIP and NBT (Sigma Chemical Co.). When a chemiluminescence detection method was chosen, anti-MHP1 was used in a 1:1,000 dilution, and goat peroxidase–coupled secondary antibody was used in a 1:5,000 dilution. Signal detection was carried out with the ECL kit (New England Nuclear, Boston, MA).

Indirect Immunofluorescence Microscopy

Yeast cells were harvested during exponential growth phase and prepared for immunofluorescence staining as described (Kilmartin and Adams, 1984). The anti–α-tubulin antibody YOL1/34 (Kilmartin et al., 1982) was used at a 1:20 dilution, and a 1:200 dilution was used for the polyclonal anti-MAP antibodies. To visualize MTs and Mhp1p, TRITC-labeled secondary antibodies (Socochim, Pully, Switzerland) were used for tubulin, and FITC-labeled anti–rabbit IgG (Socochim) were used for the polyclonal anti-MHP1 antibodies. The DNA staining dye 4′,6-diamidino-2-phenylindole (DAPI) and 0.1% *p*-phenylenediamine were added to the mounting medium to visualize the nuclear region. An alternative procedure was applied to better preserve the cytoplasmic localization of Mhp1p; the fixation and digestion of cells was 30 min each, and the time of antibody incubation was reduced to 50–60 min.

Epitope Tagging of Mhp1p

The antigenic myc-tag (Munro and Pelham, 1984) was PCR amplified, generating terminal BamHI sites, and cloned into the BamHI site located between the GAL promoter and the *MHP1* sequence on plasmid pMAC-Pst (Table II), generating pMACmyc-Pst. Constructs were sequenced to confirm correct insertion and conservation of the open reading frame (ORF). Y507 cells, transformed with plasmid pMACmyc-Pst (Tables I and II), were grown in selective medium overnight and for another 10 h in selective medium containing 1% galactose or 1% glucose. For immunofluorescence microscopy, the tagged epitope was detected with monoclonal

Published December 1, 1996

Table II. Plasmids Used in This Study

Plasmid	Description	Source or Reference
pADNS	*LEU2, 2μ*	Colicelli et al., 1989
pADN-205	205K MAP cDNA cloned into pADNS polylinker	This study
pBS-Bam	3.7-kb *MHP1* fragment, containing amino acid codons 219–1,398 and 3′–untranslated region, in pBS	This study
pET-15b	T7 expression vector containing His-tag	Studier et al., 1990
pET-C1188	820-bp *MHP1* fragment, containing amino acid codons 1,188–1,398 and 3′-untranslated region, in pET	This study
pET-N440	1,320-bp *MHP1* fragment, containing amino acid colons 1–440, in pET	This study
pMAC-80	GAL4 promoter cloned between SacI and BamHI site of polylinker of the pRS315 plasmid	This study
pMAC-Bam	3.7-kb *MHP1* fragment, containing amino acid codons 219–1,398 and 3′-untranslated region, in pMAC-80	This study
pMAC-MHP	4.2-kb *MHP1* fragment, containing amino acid codons 1–1,398 and 3′-untranslated region, in pMAC-80	This study
pMAC-PST	2.5-kb *MHP1* fragment, containing amino acid codons 561–1,398 and 3′-untranslated region, in pMAC-80	This study
pMACmyc-Pst	Antigenic myc-tag, cloned into BamHI site of pMAC-Pst at 5′-end of *MHP1* sequence	This study
pRS315	*LEU3, CEN6*	Sikorski and Hieter, 1989
Yep24	*URA3, 2μ*	Botstein et al., 1979
Yep-MHP	5.5 kb, containing *MHP1* gene in Yep24	This study

anti-myc antibodies (generous gift of Prof. T. Kreis and Dr. L. Huber, University of Geneva, Switzerland) and visualized with a secondary anti-mouse IgG fluorescein conjugate.

Disruption of MHP1

The *mhp1-Δ1* allele (see Fig. 6) was generated by excising a 1.1-kb EcoRI fragment from the *MHP1* coding region, from amino acid residues 818–1,210 (see Fig. 2 *A*), and inserting a 0.9-kb EcoRI fragment containing the *TRP1*$^+$ marker. The MHP1–TRP1 construct was excised from the plasmid with SalI (one genomic SalI site and one site in the plasmid linker) and transformed into the diploid Trp$^-$ strain Y501 (Rothstein, 1983). Trp$^+$ transformants Y502 were analyzed for correct insertion of the marker gene by PCR and Southern blot analysis. The *mhp1-Δ2::URA3* mutation was generated by inserting the *URA3*$^+$ marker between the two PstI sites at position 1667 and 1679, respectively (see Fig. 2 *A*). A 4.5-kb SalI–HindIII fragment was excised and used to generate the heterozygous Ura$^+$ cells Y105. Insertion of the marker gene was confirmed on Southern blots. *mhp1-Δ4::TRP1* was generated by cloning a PvuII fragment containing the *TRP1*$^+$ marker gene between two NcoI sites (positions −2 and 1833) within the *MHP1* gene. A 3-kb NotI–SalI fragment (both sites in the linker sequence of pBS) was excised and used to transform Y501 cells, and Trp$^+$ transformants Y521 were selected. The correct insertion of the marker gene was confirmed by PCR. The *mhp1-Δ5::HIS3* mutation was generated by excising the PstI–EcoRI fragment (from position 1667 to 3626) and replacing it with a PstI–EcoRI fragment containing the *HIS3*$^+$ marker gene. A 3.5-kb SalI–SalI fragment (one SalI site near the 5′ end of MHP1 and one SalI site in the linker sequence at the 3′ end of the *MHP1* gene) was used to transform Y501 cells, and His$^+$ transformants Y531 were selected and analyzed for insertion of the marker gene by PCR.

The *mhp1-Δ6::kan*^{r} allele was generated by PCR amplifying the *kan*^{r} gene from the plasmid pFA6-kanMX4 (Wach et al., 1994), using the primers 5′ CACTTAAATACGCAAAATATACAAGATAGCCCTACAACT-GCTCCATGCAGCTGAAGCTTCGTACGC 3′ and 5′ TTATTTAGT-ACTACTGTTCCGCGCATCCTGGATTTTGTCTAGCACGCATAGG-CCACTAGTGGAT 3′. The resulting DNA fragment contained terminal ends homologous to 45 bp flanking the respective translation start and stop sites of *MHP1*. Transformants were selected on plates containing rich medium supplemented with 100 mg of G418 per liter. Six independent transformants were obtained that contained the *mhp1-Δ6::kan*^{r} allele correctly substituted at the *MHP1* locus as analyzed by PCR.

Complementation and Overexpression Experiments

To complement the *mhp1-Δ6::kan*^{r} allele with *MHP1*, we generated pMAC-MHP. The region including nucleotides 1–670, downstream from the unique SalI site, was amplified by PCR with terminal BamHI sites and cloned into the BamHI site of pMAC-80, a derivative of pRS315 (Sikorski and Hierter, 1989), into which we had inserted the GAL promoter (Table II). The remaining 3.6 kb of the *MHP1* coding region from the SalI site at bp 752 to the 3′ end (SalI site in the multicloning site of pBS) were inserted into the SalI site, and correct orientation was determined by restriction digestion analyses. Heterozygous *mhp1*$^+$*/mhp1-Δ6::kan*^{r} cells Y561 were transformed with pMAC-MHP or pMAC-Pst (Table II), and Leu$^+$ and G418-resistant cells were sporulated and dissected on glucose- and galactose-containing plates. In 8 out of 12 tetrads, two colonies of normal size and two small colonies could be observed after 4–5 d of incubation at 30°C, with the normal-sized colonies unable to grow on G418. All small colonies were Leu$^+$ and resistant to G418. Colonies growing from individual spores were followed by microscopic inspection for 7 d. Leu$^+$ and G418-resistant cells from glucose plates were grown in liquid medium containing either glucose or galactose, and aliquots were taken after 4 and 20 h of growth and prepared for immunofluorescence.

Overexpression of the 3′ half of *MHP1*, designated *mhp1-Δ3*, was performed with the clone pMAC-Pst. The *mhp1-Δ3* allele was generated by cloning the region from bp 1,769–4,339 of the *MHP1* gene between the PstI and SalI sites of pMAC-80 (Table II). The correct insertion was verified by restriction analysis. Y501 and Y502 cells were transformed, and Leu$^+$ or Leu$^+$ Trp$^+$ lines were generated and designated Y505 and Y506, respectively. pMAC-Bam was generated by cloning a BamHI–PstI fragment (bp 657–1,684) of *MHP1* between the BamHI and PstI sites of pMAC-Pst. Y501 cells were transformed with pMAC-Bam and Leu$^+$ transformants were designated Y508. For phenotypic analysis, the cells were grown in selective medium overnight, and 5 to 20 h in selective medium and 2% galactose.

Rescue experiments of the *mhp1-Δ1* deletion mutation were attempted with the 4.5-kb cDNA of the *Drosophila* 205K MAP (Irminger-Finger et al., 1990), which was cloned into the NotI site of the yeast multicopy expression vector pADNS (Colicelli et al., 1989), containing the alcohol dehydrogenase (ADH) promoter and the selectable marker *LEU2*$^+$, generating plasmid pADN-205 (Table II). The heterozygous *mhp1*$^+$*/mhp1-Δ1* cells Y502 and *mhp1*$^+$*/mhp1-Δ6* cells Y561 were transformed with the resulting plasmid pADN-205. Leu$^+$ transformants were selected and used for tetrad analysis. Silencing of the ADH promoter was performed in medium containing 2% galactose instead of glucose. Cell growth was quantified by growing cells for 12–20 h in glucose, and then the OD_{600} was measured. Cells were diluted to an OD_{600} of 0.05 and growth was monitored in glucose and in galactose.

Results

Cloning of MHP1

To clone genes encoding yeast MAPs, a cDNA expression library was screened with a previously produced antibody raised against the *Drosophila* 205K MAP (Goldstein et al., 1986). The positive cDNA phage 205.41a was used as hybridization probe to isolate the genomic clone F2B8 (Fig. 1 *A*). DNA fragments from different regions within F2B8 were used to determine the size of the *MHP1* transcripts on Northern blots (Fig. 1 *A*, probes 1 and 2). Both probes hybridized to an mRNA of 4,500 nucleotides. DNA sequence analysis of the transcribed region, including probe 1 and 2, revealed an ORF coding for 1,398 amino acids

Published December 1, 1996

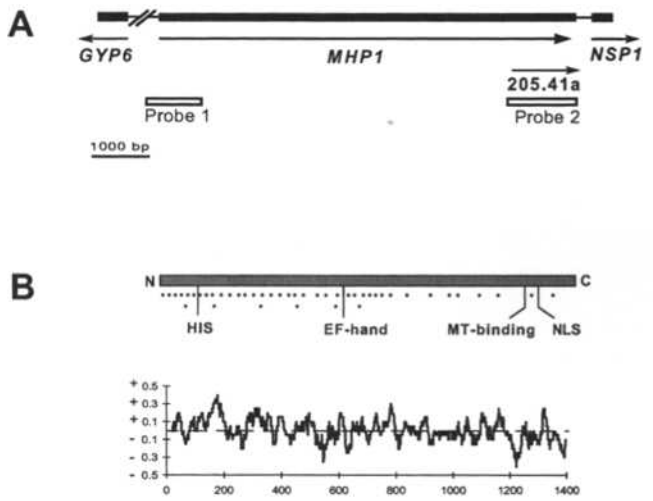

Figure 1. *MHP1* gene structure and diagram of protein organization. (*A*) Organization of genomic clone F2B8 with relative localization of the *MHP1* coding region between *GYP6* and *NSP1*, as well as the size and relative location of λgt11 cDNA clone 205.41a, are shown. (*Arrows*) Directions of transcription. Probe 1 and 2 were used to probe Northern blots. (*B*) Schematic diagram of the organization of Mhp1p. (*Asterisks*) Potential phosphorylation sites. *HIS*, *EF-hand*, *MT-binding*, and *NLS* refer to the positions of motifs discussed in the text. The density of positively and negatively charged amino acids in a sliding window of 20 residues was calculated and plotted against the amino acid sequence.

preceded by a putative CAAT box and a TATA box at positions −52 and −27, respectively (Fig. 2 *A*). The coding region of *MHP1* is identical with ORF YJL042W on chromosome X and is separated by 344 noncoding bp from *NSP1* (Hurt, 1988) and ~1,300 bp from *GYP6* (Strohm et al., 1993).

DNA and Protein Sequence Analysis

No significant homologies with other proteins were found when the EMBL and Swissprot databases (release May 1996) were searched with the *MHP1* sequence. From amino acid residues 128–137, nine histidines are encoded that could have a function in metal binding. With sequence analysis programs for the detection of specific motifs, a possible EF hand motif was identified between amino acid residues 615 and 629 (Fig. 2 *A*). When the *MHP1* protein sequence was compared directly with protein sequences of known MAPs using PILEUP, MAP4, MAP2, tau, and Mhp1p could be aligned and showed a significant similarity in a region close to the COOH terminus, including residues 1,211–1,266 in Mhp1p (Fig. 2 *B*). Within this region, Mhp1p has between 23 and 32% identity or between 33 and 38% similarity with the sequences of the other MAPs. The highest similarity score was found with MAP4, and the lowest with tau. Included in this region is (from residues 1,234–1,266 of Mhp1p) one repeat of the AP motif common to tau, MAP2, and MAP4 (Lee et al., 1988; Lewis et al., 1988; Aizawa et al., 1990; Chapin and Bulinski, 1991; West et al., 1991). Some 50 residues downstream from the putative MT-binding motif, a nuclear localization signal (NLS) consensus sequence (Roberts, 1989) is present (Fig. 2 *A*).

MHP1 encodes a hydrophilic protein, with a calculated isoelectric point (pI) of 6.9, but is composed of alternating basic and acidic regions within which the calculated pI values range from 10–12 and from 4.5–5, respectively (Fig. 1 *B*). The highest concentration of charged amino acids is observed within acidic and basic regions near the COOH-terminal end of Mhp1p. The NH_2-terminal and the COOH-terminal regions of Mhp1p are very proline rich, typical of extended protein structures, but between residues 1,070 and 1,150 a propensity for the formation of α helices is predicted (Chou and Fasman, 1978; Garnier et al., 1978).

A total of 52 potential phosphorylation sites for the cAMP-dependent kinase (Edelmann et al., 1987), the calcium-phospholipid–dependent kinase (Gonzales et al., 1989), the Ca^{2+}-calmodulin–dependent kinase (Pearson et al., 1985), and the casein kinase II (Diaz-Nido et al., 1988) are situated within the NH_2-terminal two-thirds of Mhp1p, but only two potential sites are localized within the COOH-terminal domain (residues 1,201–1,398) of the protein (Figs. 1 *B* and 2 *A*).

Identification of Mhp1p with Anti-MHP1 Antibodies

To obtain Mhp1p-specific antisera, clone pET-C1188 encoding amino acids 1,188–1,398 was expressed in *E. coli*, and antibodies were generated against the His-tagged 36-kD protein C1188p. The antiserum was tested on Western blots and recognized the purified samples of C1188p and C1188p in protein lysates of induced bacterial cultures. On Western blots of whole cell extracts from *S. cerevisiae*, a 200-kD protein as well as smaller proteins of ≤46 kD were consistently recognized by anti-MHP1 (Fig. 3 *A*; *Y501* and *Y502*) when 20 μg of total protein extract was loaded.

The amount of anti-MHP1 reactive protein is reduced in *mhp1*$^+$/*mhp1-Δ1* heterozygous cells Y502 compared with mhp1$^+$ cells Y501 (Fig. 3 *A*). When an equal amount of protein from Y509 cells overproducing Mhp1p from a multicopy plasmid was loaded, the 200-kD protein was substantially increased on Western blots, but also a protein of 150 kD could be detected. The full-length *MHP1* gene expressed in *E. coli* also migrates at 200 kD, supporting the conclusion that full-length Mhp1p is identical with the 200-kD band (data not shown). Less intense staining was observed for proteins of 230, 90, 60, and 46 kD. After longer exposure times, the same patterns of proteins were observed in the protein extracts from Y501 and Y502 cells. To test the specificity of the antibody reaction, competition experiments were performed using purified C1188p. The addition of 1–10 μg/ml, purified C1188p was tested, and 5 μg/ml was found to be sufficient to compete the antibody recognition of Mhp1p on Western blots. When 5 μg/ml purified C1188p was added during the antibody incubation, the 200-kD as well as the other proteins observed in Y509 cells could be completely competed with C1188p (Fig. 3 *A*, *b*). These proteins presumably contain the COOH terminus against which anti-MHP1 was raised, and are either isoforms of Mhp1p and/or degradation products, although the caveat remains that anti-MHP1 might recognize an epitope that is present on other proteins. The observed size of 200 kD for Mhp1p is considerably larger than its calculated molecular mass of 154 kD, but it could result from phosphorylation and abnormal migration as a result of the acidic portions of the protein.

Published December 1, 1996

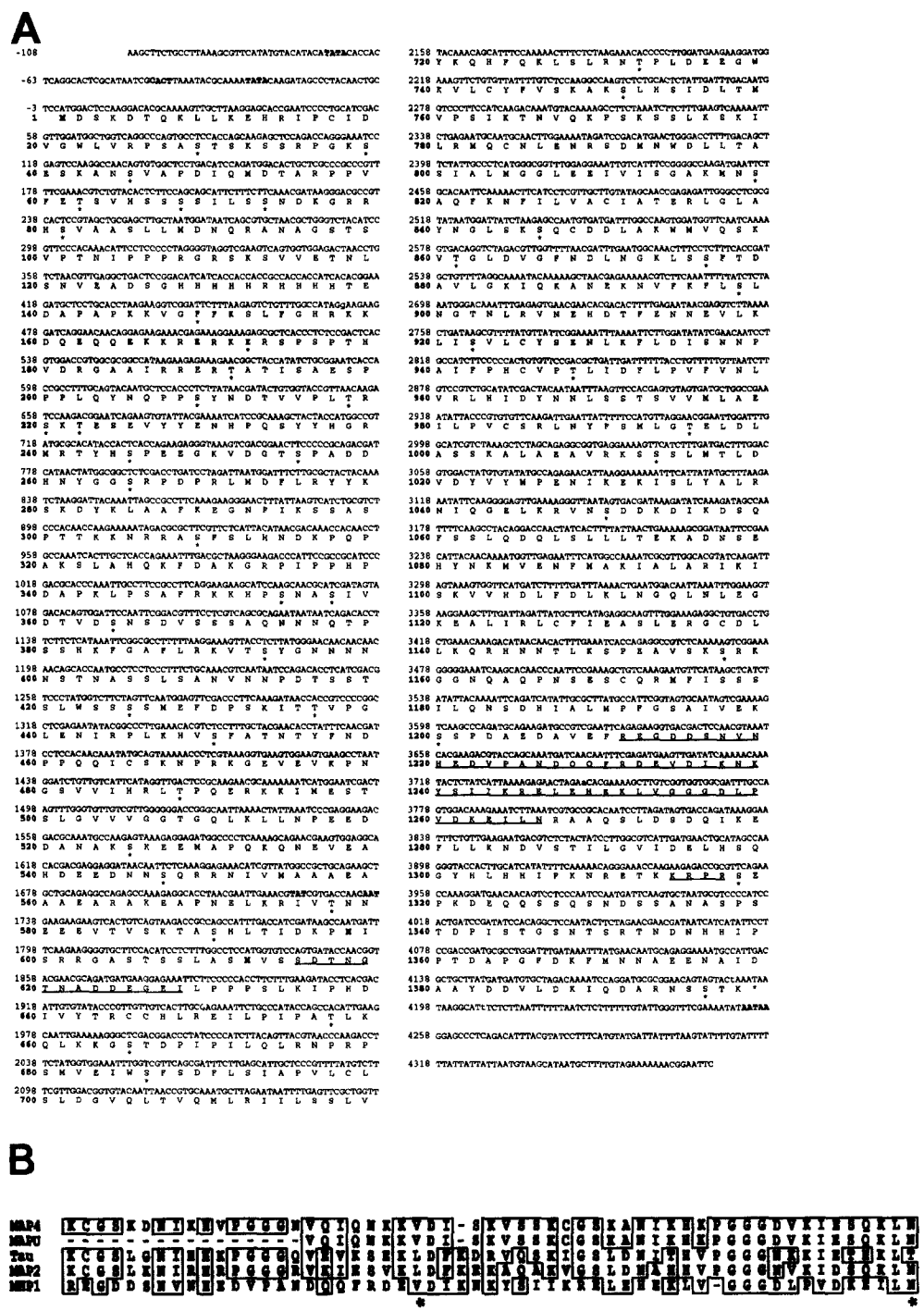

Figure 2. DNA sequence and predicted protein sequence of *MHP1*. (*A*) DNA sequence of the *MHP1* gene and predicted amino acid sequence are presented. Bold letters indicate the TATA and CAAT sequences, a polyadenylation signal, the first methionine initiation codon, and potential initiation codons of the *mhp1-Δ2::URA3* mutation (see Fig. 6). Potentially phosphorylated amino acids are indicated by an asterisk below the residue. The putative EF hand motif (beginning at residue 615), the region homologous to MAP2, MAP4, and tau (from residues 1,211–1,266), and the potential NLS (residues 1,314–1,317) are underlined. Sequence data are available from EMBL/GenBank/DDBJ under accession number X84256. (*B*) Protein sequence alignment of AP sequences of different MAPs. Protein sequences of Mhp1p (1,211–1,266), human (233–288) and mouse (222–277) tau, mouse MAP2 (1,709–1,764), human (1,007–1,062) and mouse (980–1,035) MAP4, and bovine MAP U (944–977) are aligned. Amino acids, identical or similar (E/D, K/R, I/L/V) in at least three proteins, are boxed. The alignment corresponding to the AP repeat is bordered with asterisks.

A 200-kD protein plus a 180-kD protein were also reactive with the anti-205K MAP antiserum originally used for the screening of the λgt11 expression library (Fig. 3 *B*, lanes *1* and *2*), but only the 200-kD protein copurified with yeast tubulin on a DEAE column (Bellocq et al., 1992). When heat-stable yeast proteins were tested with anti-MHP1 and anti-205K MAP, the 200-kD protein was also detected by both antisera (Fig. 3 *B*, lanes *3* and *4*).

Mhp1p Has MT-binding Activity In Vitro

To determine whether Mhp1p binds to MTs in vitro, MT-binding and cosedimentation experiments were carried out. Total yeast proteins were incubated with preformed MTs and centrifuged, and supernatant and pellet fractions were analyzed on Western blots probed with anti-MHP1 (Fig. 4 *A*, *a*). The anti-MHP1–reactive 200-kD protein was coprecipitated with MTs and could be identified on Western blots. To localize the MT-binding activity within the *MHP1* sequence, deletion-bearing clones were in vitro transcribed and translated, and aliquots of the in vitro translation reactions were tested in MT-binding assays. The COOH-terminal fragment C1188 coprecipitated with preformed MTs with >80% of the counts of the transla-

Published December 1, 1996

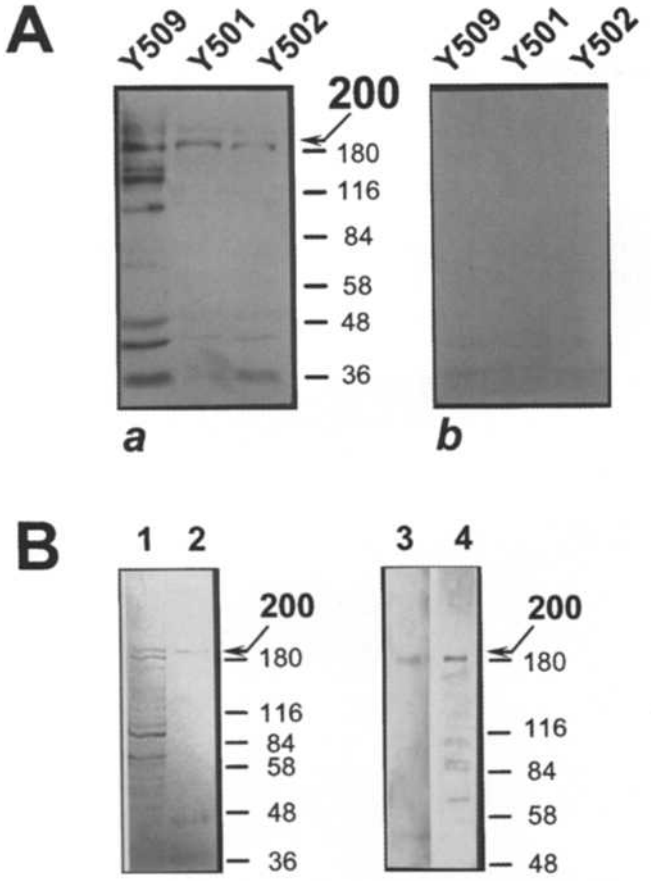

Figure 3. Identification of Mhp1p on Western blots. (*A*) Western blot of total yeast extracts from homozygous mhp1$^+$ cells, Y501, heterozygous cells Y502, and cells overproducing Mhp1p, Y509. (*a*) 7.5% SDS gels were loaded with the equivalent of 50 μg of yeast cells, blotted and probed with affinity-purified anti-MHP1. (*b*) An identical Western blot as in *a* was prepared and used for an antigen competition assay using purified C1188p. (*B*) Western blot of total yeast protein extracts probed with anti-C1188p and anti-205K MAP antibodies. 10 μg total yeast protein extract (lane *1*) and 5 μg of protein copurified with tubulin on a DEAE column (lane *2*) were loaded and probed with anti-205K MAP. (*Arrows*) Position of the 200-kD protein that is very low in abundance but reproducibly recognized by anti-205K MAP; a representative Western blot out of five independent experiments is shown. Sizes of molecular weight standards are indicated on the right side. Heat-stable proteins of an equivalent of 50 μg of Y501 cells were loaded and probed with anti-205K MAP (lane *3*) and anti-MHP1 (lane *4*).

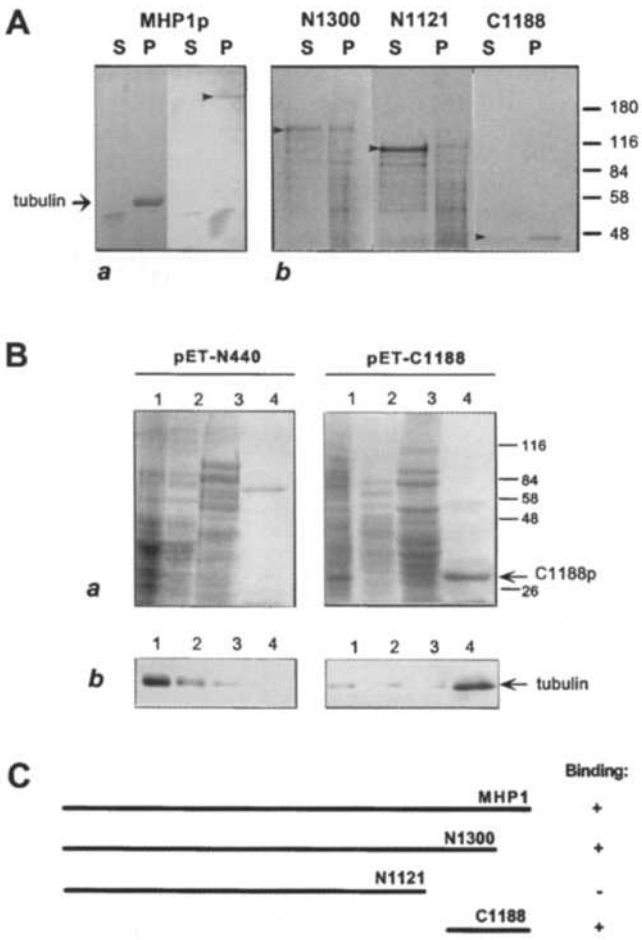

Figure 4. Microtubule-binding assays. (*A*) MT-binding assays performed with preformed MTs from purified pig tubulin. (*a*) The binding of wild-type Mhp1p was tested using a total protein extract from Y509 cells incubated with preformed MTs and subsequent precipitation of the macromolecules. Aliquots of the supernatant (*S*) and pellet (*P*) fractions were analyzed by PAGE and tested on Western blots with anti-MHP1: PonceauS staining (*left*) and antibody staining (*right*). The 200-kD Mhp1p (*arrow*) is not very abundant but could be reproducibly detected in several independent experiments. (*b*) The MT-binding activity of different truncation products generated by in vitro transcription and translation of *MHP1* deletion-bearing clones. MT-binding reactions were precipitated, and supernatant (*S*) and pellet (*P*) fractions were analyzed by PAGE. The autoradiography of the gel is shown. (*B*) Tubulin-binding assay using His-tagged C1188p. Protein extracts from bacteria transformed with pET-N440 or pET-C1188 were loaded onto Ni-columns. Total protein extracts from yeast were applied to the column to test whether tubulin could be retained. Samples were analyzed by PAGE and Western blotting, with the Coomassie-stained gel shown in *a* and the Western blot probed with anti-α tubulin in *b*. Gels were loaded with aliquots from load (lane *1*), flow-throw (lane *2*), wash (lane *3*), and elution (lane *4*) fractions. (*C*) The relative sizes of the translation products used in the MT-binding assays are shown schematically. More than 80% of radioactive protein in the pellet lane was considered to be MT binding (+), >80% in the supernatant was not binding (−), and 50% in the supernatant and 50% in the pellet fraction was (+/−) binding.

tion reaction in the pellet fraction, which was considered specific binding, while the N1121 protein, terminating at residue 1,121, showed virtually no binding and >80% of the radioactivity remained in the supernatant (Fig. 4 *A*, *b*). Traces of radioactive protein in the pellet were considered as background, since similar amounts were observed in control experiments with unrelated proteins. The N1300 construct, terminating after residue 1,300, showed an intermediate binding with approximately the same amount of radioactive protein in the pellet and in the supernatant fraction, although it contained the sequence homologous to the tau-repeat. These experiments suggest that the COOH-terminal end of Mhp1p that is contained in C1188

Published December 1, 1996

but not in N1300 may be needed for efficient binding or, alternatively, that the folding of a putative binding domain may be disturbed in the N1300 deletion.

To confirm by an independent approach that the COOH-terminal domain of Mhp1p contains a region that promotes MT-binding, we took advantage of the His-tag purification procedure of proteins expressed from the pET-15b vector in *E. coli.* We used the COOH-terminal peptide C1188p, immobilized on Ni-columns, to identify proteins that interact with this region of Mhp1p. Ni-columns containing bound C1188p were saturated with crude yeast protein extracts in MT-binding buffer, washed, and then eluted with the standard metal-chelation buffer. Several proteins bound to the C1188p-column. A 48-kD protein was identified as tubulin on Western blots probed with antibodies against α- or β-tubulin (Fig. 4 *B*). In control experiments, crude yeast protein extracts were loaded on a Ni-column that was preabsorbed with either a protein extract from bacteria not expressing exogenous genes or a protein extract from bacteria transformed with the His-

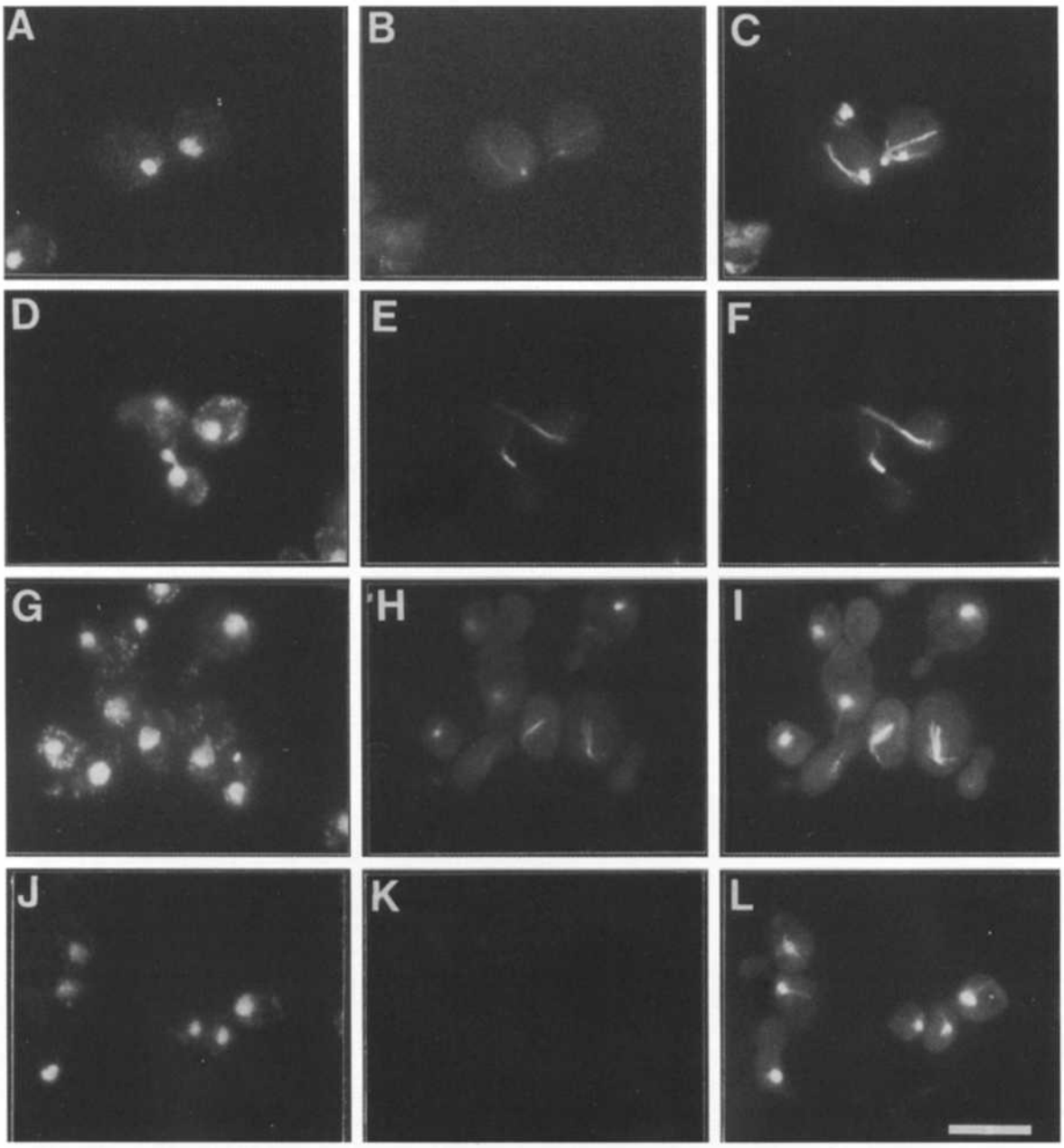

Figure 5. Immunolocalization of Mhp1p. Localization of Mhp1p in interphase cells is shown with DAPI staining (*A*), anti-MHP1 staining (*B*), anti-tubulin staining (*C*), and in a pair of dividing cells with DAPI (*D*), anti-MHP1 (*E*), and anti-tubulin staining (*F*). A representative field of Y507 cells expressing myc-tagged Mhp1p is shown with DAPI staining in *G*, anti-myc in *H*, and anti-tubulin staining in *I*. In an anti-myc control experiment, Y501 cells were stained with DAPI (*J*), anti-myc (*K*), and anti-tubulin (*L*). Fluorescein-conjugated secondary antibodies were used against the rabbit anti–MHP1 and the mouse anti–myc antibodies. Rhodamine-conjugated antibodies were used against the rat anti–α-tubulin antibody YOL1/34. Bar, 4.5 μm.

Published December 1, 1996

tagged NH_2-terminal part of Mhp1p, including amino acid residues 1–440. In both cases, some proteins were bound, but the binding of tubulin or MTs was only observed after preabsorption with the bacterial extract producing C1188p (Fig. 4 *B*, *right*). Hence, the MT-binding activity was confirmed to reside principally in the COOH-terminal region of Mhp1p containing the AP-homologous sequence.

Immunolocalization of Mhp1p

Immunolocalization of Mhp1p with anti-MHP1 was carried out in Y501 and Y509 cells that carry *MHP1* from a multicopy plasmid (Table II). Less intense staining was observed in Y501 cells than in Y509 cells that are presented (Fig. 5, *A–C*). Cytoplasmic MTs were decorated in ~60% of interphase cells (Fig. 5, *A–C*). In mitotic cells, short metaphase spindles as well as elongating spindles were stained (Fig. 5, *D–F*). Cytoplasmic staining was also observed in Y509 cells when an altered fixation and labeling procedure was applied (see Materials and Methods). Immunolocalization of Mhp1p in cells transformed with a myc-tagged *MHP1*, on the plasmid pMACmyc-Pst (Table II), confirmed the localization of Mhp1p on MTs (Fig. 5, *G–I*). No staining was observed with anti-myc antibodies in Y501 cells (Fig. 5, *J–L*), demonstrating that anti-myc staining was not due to fluorescence spill-over.

MHP1 Is Essential for Cell Growth

Since Mhp1p was shown to bind to MTs in vitro, it was of interest to determine whether MT structure or function was disturbed in cells lacking *MHP1*. We constructed a series of disruption alleles of *MHP1* by replacing different regions of the ORF with marker genes (Fig. 6 *A*). Deletion of the entire coding region of *MHP1* (*mhp1-Δ6::kan*^{r}) was performed in diploid Y501 cells, and tetrads of six independent transformants were dissected. The *mhp1-Δ6::kan*^{r} mutation led to lethality, and the kan$^+$/kan$^-$ phenotype segregated 2:2 in all complete tetrads, the surviving spores being unable to grow on G418. The deletion of a COOH-terminal region from amino acids 818–1,210 also resulted in lethality in haploid cells (*mhp1-Δ1::TRP1*), indicating

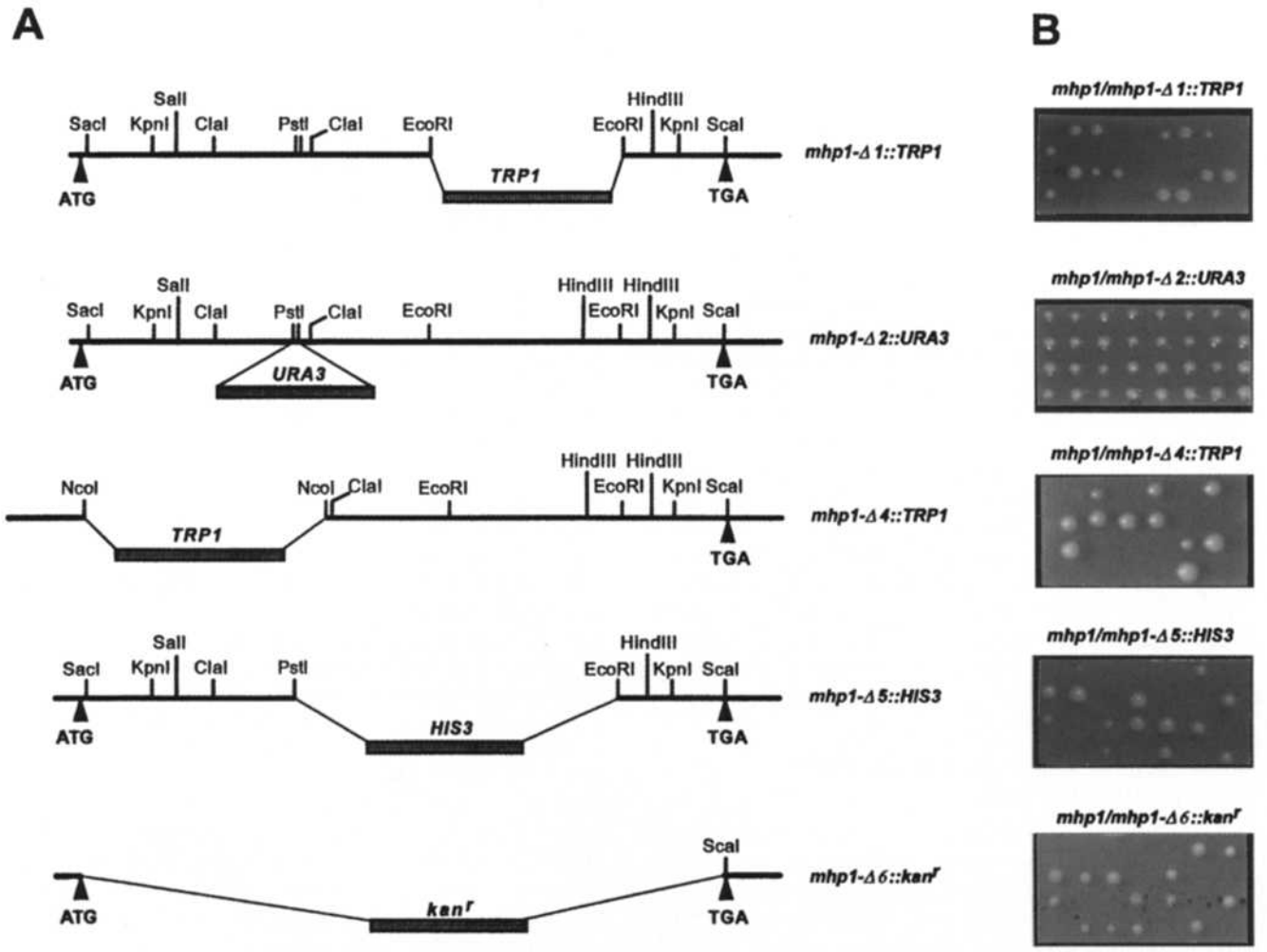

Figure 6. MHP1 disruption mutations. (*A*) Restriction maps of the different disruption alleles. The relative sites of the ATG initiation codon and the TGA stop codon are indicated. Note the presumed ATG translation start codon (see Fig. 2 *A*), which allows translation downstream from the *URA3*$^+$ insertion in the *mhp1-Δ2::URA3* mutation, absent in the *mhp1-Δ4::TRP1* mutation as well as in the *mhp1-Δ5::HIS3* mutation. The region downstream from the *URA3*$^+$ insertion in the *mhp1-Δ2::URA3* mutation was cloned into the inducible plasmid pMAC-80 and designated *mhp1-Δ3*. (*B*) Tetrad analyses of cells heterozygous for the alleles indicated in *A*.

Published December 1, 1996

that the NH_2-terminal 818 amino acids encoded on the *mhp1-Δ1::TRP1* allele are not sufficient for viability.

Surprisingly, the interruption of the ORF after amino acid 558 by the insertion of the *URA3*$^+$ marker gene led to viable haploid cells (Fig. 6). Tetrad analysis of the heterozygous diploid strain *mhp1*$^+$*/mhp1-Δ2::URA3*, Y105, resulted in four viable spores, the Ura$^+$/Ura$^-$ phenotype segregating 2:2 and the *mhp1-Δ2::URA3* haploid cells Y106 growing only slightly slower than the wild-type cells. When we analyzed the *MHP1* mRNA in wild-type and *mhp1-Δ2::URA3* disrupted cells, we found that the mutant cells expressed two transcripts (Fig. 7 *A*), a 1.8-kb mRNA covering the *MHP1* 5′ sequences and a 2.7-kb mRNA covering *MHP1* 3′ sequences, while wild-type cells expressed a single 4.5-kb mRNA. This 4.5-kb transcript is not observed in the disrupted haploid *mhp1-Δ2::URA3* cells. A weak hybridization of a 2.8-kb RNA is visible in Y501 cells that might be a second *MHP1* transcript or a nonspecific cross-hybridization. These results suggest that *MHP1* function can be obtained when NH_2-terminal and COOH-terminal sequences of *MHP1* are expressed from separate transcripts. Analysis of the proteins expressed in wild-type and *mhp1-Δ2::URA3* cells on Western blots (Fig. 7 *B*) shows that in wild-type cells, a 200-kD protein and bands of 150, 90, and 46 kD react with anti-MHP1, while in *mhp1-Δ2::URA3* haploid cells, no proteins >90 kD can be detected.

To further test the hypothesis that sequences downstream of the *URA3*$^+$ insertion were expressed spontaneously in the *mhp1-Δ2::URA3* allele, we generated deletion alleles *mhp1-Δ4::TRP1* (deletion of the first 613 amino acids) and *mhp1-Δ5::HIS3* (deletion of the region encoding amino acids 557–1,210) that do not contain the two presumed ATG translation initiation codons at positions 1792 and 1839, respectively. Both alleles proved to be lethal.

The progeny of *mhp1-Δ1::TRP1*, *mhp1-Δ4::TRP1*, *mhp1-Δ5::HIS3*, or *mhp1-Δ6::kan*^{r} cells could germinate and go through a few cell divisions, but they died at stages of 8 to 32 cells. The time needed for germination was variable for different spores and explains the size differences of the colonies (Fig. 6 *B*). The heterozygous cells showed a reduced growth rate in rich medium. Analysis of asynchronously growing Y502 and Y561 cells by DAPI and antitubulin staining showed 12% of the cells with short or long spindles and divided nuclei, compared with 2–3% routinely observed for wild-type cells under the same conditions, indicating that they are arrested or slowed during mitosis (data not shown).

Altered MT Phenotypes Induced by MHP1 Overexpression Mutations

Since the heterozygous deletion mutations of *MHP1* showed a gene dosage effect, we investigated whether overexpressed *MHP1*, or deletion-bearing alleles of *MHP1*, would lead to a dominant phenotype. Y509 cells that express *MHP1* constitutively from a multicopy plasmid (pYEP-MHP) exhibit a reduced growth rate (Fig. 8 *A*). The analysis of MT structures in asynchronously growing Y509 cells showed that the amount of cells with elongated spindles and divided nuclei was <1%, while the parental strain Y501 grown under similar conditions contained 2–3% of

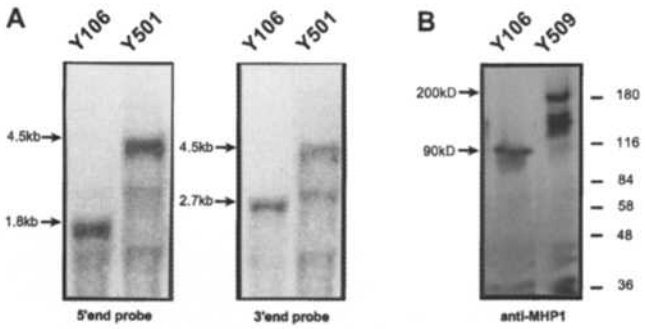

Figure 7. Analysis of the *mhp1-Δ2* mutation. (*A*) Northern blots were probed with a 700-bp probe from the 5′ end and a 600-bp probe from the 3′ end of *MHP1* (see Fig. 1 *A*). In *mhp1-Δ2::URA3* haploid cells Y106, the 5′-end probe and the 3′-end probe detected different mRNAs (*arrows*). In wild-type cells Y501, a 4.5-kb RNA was detected with both probes. (*B*) Western blot of total protein from *mhp1-Δ2::URA3* haploid cells (*Y106*) and diploid Y509 cells probed with anti-MHP1. In *mhp1-Δ2::URA3* haploid cells, anti-MHP1 reacts with a 90-kD protein compared with a 200-kD protein and smaller proteins in mhp1$^+$ cells, Y509.

cells with short or long spindles and divided nuclei. In addition, Y509 cells showed an increased cell volume (150–200% of diploid wild-type cells), many abnormally long MT filaments emanating from one SPB, increased nuclear DNA staining, and small patches of DAPI-stained material observable in the cytoplasm (Fig. 8 *B*, *a*). In 6% of the cells, bud formation occurred but no spindle was formed. The increase in length and number of MTs in Y509 cells, as a consequence of increased expression of *MHP1*, is compatible with the role of Mhp1p as a positive regulator of MT stability.

A different phenotype could be induced by the overexpression of the COOH-terminal portion of Mhp1p. The region encoded on pMAC-Pst (Table II), designated *mhp1-Δ3*, was transformed into homozygous mhp1$^+$ cells and into *mhp1*$^+$*/mhp1-Δ1* heterozygous cells, generating Y505 and Y506 cells, respectively. Cells were grown in medium containing either glucose, galactose, or raffinose (a sugar derepressing the GAL promoter and leading to less expression than galactose). The induction of *mhp1-Δ3* was monitored on Western blots, and the expression of a 90-kD protein, as had been identified in *mhp1-Δ2* cells under conditions of unstimulated expression (see Fig. 7 *B*), could be observed in Y505 and Y506 when cells were grown in galactose or raffinose (data not shown).

The expression of *mhp1-Δ3* provoked a negative effect on growth rate. While control cells Y502 reached saturation after ~24 h with a doubling time of 3 h in media containing galactose, for transformed Y505 and Y506 cells, longer times were required to reach saturation when grown in galactose-containing media, with generation times of 4.5 and 6 h, respectively. When media containing increasing amounts of galactose and decreasing amounts of glucose, or the partial inducer raffinose, were used, the growth rates of Y505 and Y506 cells were correlated with the galactose or raffinose content in the media.

To determine the consequence of the expression of *mhp1-Δ3* on MT structure and function, we analyzed asynchronously growing cultures by immunofluorescence mi-

Published December 1, 1996

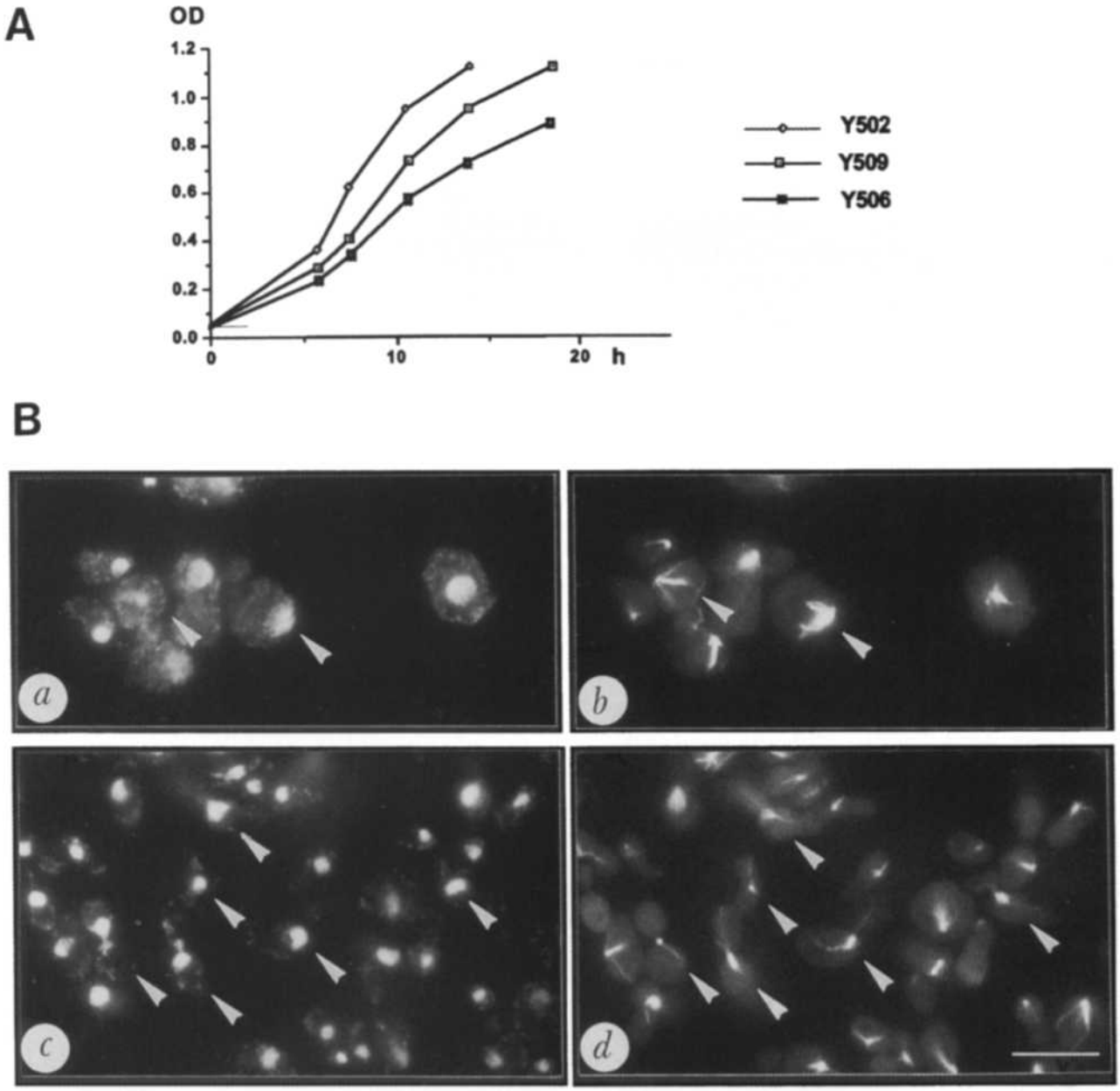

Figure 8. Overexpression of the *MHP1* gene and of the *mhp1-Δ3* allele. (*A*) Growth rate of Y502, Y509, and Y506 cells was monitored by measuring the OD_{600} (OD_{600} at time 0 was 0.05) in selective medium containing 2% galactose. (*B*) Analysis of MT structure in Y509 (*a* and *b*) and Y506 (*c* and *d*) cells. The formation of long cytoplasmic MTs (*arrowheads*) can be observed in Y509 cells overexpressing *MHP1*. The accumulation of cells with short spindles (*arrowheads*) is shown in a typical field of Y506 cells overexpressing the *mhp1-Δ3* allele (*c* and *d*). Nuclei are visualized by DAPI staining (*a* and *c*), and MTs by anti-tubulin staining (*b* and *d*). Bar, 4.5 μm.

croscopy with anti-tubulin staining. When Y505 and Y506 cells were grown in raffinose or galactose, their progression through mitosis was slowed down in various stages of mitosis. With the activation of the GAL10 promoter, an accumulation of cells with large buds, monopolar or short bipolar spindles, unseparated nuclei within the mother cells or at the bud neck, and cytoplasmic MTs extended into the daughter cells (but very sparse or not detectable) could be observed (Fig. 8 *B*), while the number of cells with separated nuclei and long spindles decreased with increased expression of *mhp1-Δ3*. The percentage of cells exhibiting this phenotype was correlated with the level of *mhp1-Δ3* expression (higher when cells were grown in galactose than when grown in raffinose) and with the time after induction (Table III). After 20 h of induction, 60% of the Y505 cells were large budded and had short or monopolar spindles formed. Only 5% of the cells were large budded with elongated spindles and nuclear migration that had proceeded into the bud. In the heterozygous Y506 cells, we observed 78% large-budded cells of which 73% had short or monopolar spindles. The comparison of the cell cycle arrest phenotype of Y506 cells after different times of *mhp1-Δ3* induction demonstrates that a short bipolar spindle can be formed, but spindle elongation might

Published December 1, 1996

be hampered. In control cells transformed with pMAC-MHP overexpressing the entire *MHP1* gene or transformed with pMAC-80 (Tables I and II), no such phenotypes were observed. The NH_2-terminal 561 amino acid residues of *MHP1* therefore appear to be required for the function of Mhp1p during progression through anaphase.

MHP1 Null Allele Complemented with MHP1 and with mhp1-Δ3

To further characterize the null phenotype of the *MHP1* deletion alleles, we have performed rescue experiments with *MHP1* on plasmids under the control of inducible promoters. pMAC-MHP contains full-length *MHP1* under the GAL10 promoter, while pMAC-Pst contains the 3′ region of the gene designated *mhp1-Δ3*. With both plasmids, the lethal phenotype of the haploid *mhp1-Δ6::kan*^{r} cells could be partially rescued, giving rise to small colonies (Fig. 9 *A*). The fact that *mhp1-Δ3* could also partially compensate for the null mutation of *MHP1* is consistent with the finding that the insertion mutation *mhp1-Δ2* is viable, and confirms that the expression of the region encoding amino acids 560–1,398 is sufficient for vegetative growth. With both plasmids, rescue could only be observed when dissections were carried out on plates containing glucose, and tetrads dissected on plates containing galactose gave rise to only two colonies of normal size. Microscopic inspection of the spores on galactose-containing plates, at intervals of 1 d, showed that all cells sporulated and divided initially with the same doubling times until they reached the ~16–32 cell stage. Two colonies slowed down in their doubling time and finally stopped growing. We presume that the overproduction of Mhp1p under the GAL10 promoter was toxic to the cells, and that leaky expression of *MHP1* from the GAL10 promoter allowed reduced transcription and translation of *MHP1* and *mhp1-Δ3* in the small-sized colonies growing on glucose plates.

MHP1 Expression Is Required for Sufficient Formation of MTs

To examine the MT phenotype in the *MHP1* null allele, we have generated haploid *mhp1-Δ6* cells Y564, complemented with inducible *MHP1* on the plasmid pMAC-MHP. When Y564 cells were grown under noninduced conditions, Mhp1p was below detectable levels when tested on Western blots or by immunofluorescence analysis. However, since it became apparent that leaky expression of *MHP1* from the GAL10 promoter was sufficient for cell growth (Fig. 9 *A*), we analyzed the phenotype of Y564 cells after growth in glucose and galactose. Immunostaining with anti-tubulin antibodies and DAPI revealed that the rescued haploid *mhp1-Δ6::kan*^{r} cells contained few MTs (Fig. 9 *B*). At least 15% of the cells formed small or large buds, but only weak staining of mitotic spindles could be observed. However, the diffuse staining of tubulin in the cytoplasm was increased. When cells were grown for several hours in galactose, which led to a reduced growth rate, long MT fibers were formed in 5% of the cells, in ~10% of the cells weak staining was observed, and in the majority of cells neither MT nor DAPI staining was detectable. The parental diploid cells Y562 prepared under identical conditions showed intense MT staining in interphase and mitotic cells (Fig. 9 *B*). The comparison of the MT morphology of the null mutant, wild-type cells, and cells expressing elevated levels of *MHP1* suggests that Mhp1p is required for the formation or stabilization of MTs and that the gene dosage of *MHP1* is crucial for correct MT function.

Partial Rescue of Lethal Alleles of MHP1 with the Drosophila 205K MAP

Since Mhp1p could be considered as a MAP based on in vitro MT-binding assays, it was important to test whether the lethal phenotype of the *mhp1-Δ1* or *mhp1-Δ6* alleles could be rescued by the expression of another MAP. Candidate proteins were the *Drosophila* 205K MAP because of its immunological relationship with Mhp1p, and the mammalian MAP4 because of its sequence homology with Mhp1p. Heterozygous *mhp1*$^+$*/mhp1-Δ1* and *mhp1*$^+$*/mhp1-Δ6* cells were transformed with the 205K MAP cDNA under the control of the ADH promoter, and Leu$^+$ transformants were sporulated and tetrads dissected. In 8 out of 12 dissected tetrads, two colonies of normal size and two small colonies were seen after 5 d of incubation at 30°C (Fig. 10 *A*, *inset*), the two small colonies being Leu$^+$ Trp$^+$ or Leu$^+$ G418 resistant, respectively. Dissection of the Y502 and Y561 strains under identical conditions reproducibly showed that all complete tetrads developed only two viable spores after 5 d of incubation at 30°C. In tests of the ability of the mouse MAP4 cDNA, cloned into the same plasmid pADNS, to compensate the *mhp1-Δ1* muta-

Table III. Cell Cycle Arrest of mhp1-Δ3 Mutant

Cell line	Time of induction*	Unbudded	Large bud		
		Mononucleate	Monopolar spindle	Short spindle	Elongated spindle
	h		*% (n)*		
Y501	0	97 (118)	0	0	3 (4)
Y501	4	96 (205)	0	2 (4)	2 (4)
Y501	12	96 (160)	0	1 (2)	3 (5)
Y501	20	97 (174)	0	1 (2)	2 (4)
Y506	0	91 (153)	0	2 (3)	7 (12)
Y506	4	45 (87)	14 (25)	24 (46)	18 (35)
Y506	12	39 (37)	14 (13)	33 (31)	14 (13)
Y506	20	22 (17)	25 (19)	48 (35)	5 (4)

*Time of induction indicates hours of growth in galactose-containing medium.
Numbers in other columns correspond to percentages and numbers of cells observed with the indicated phenotype.

Published December 1, 1996

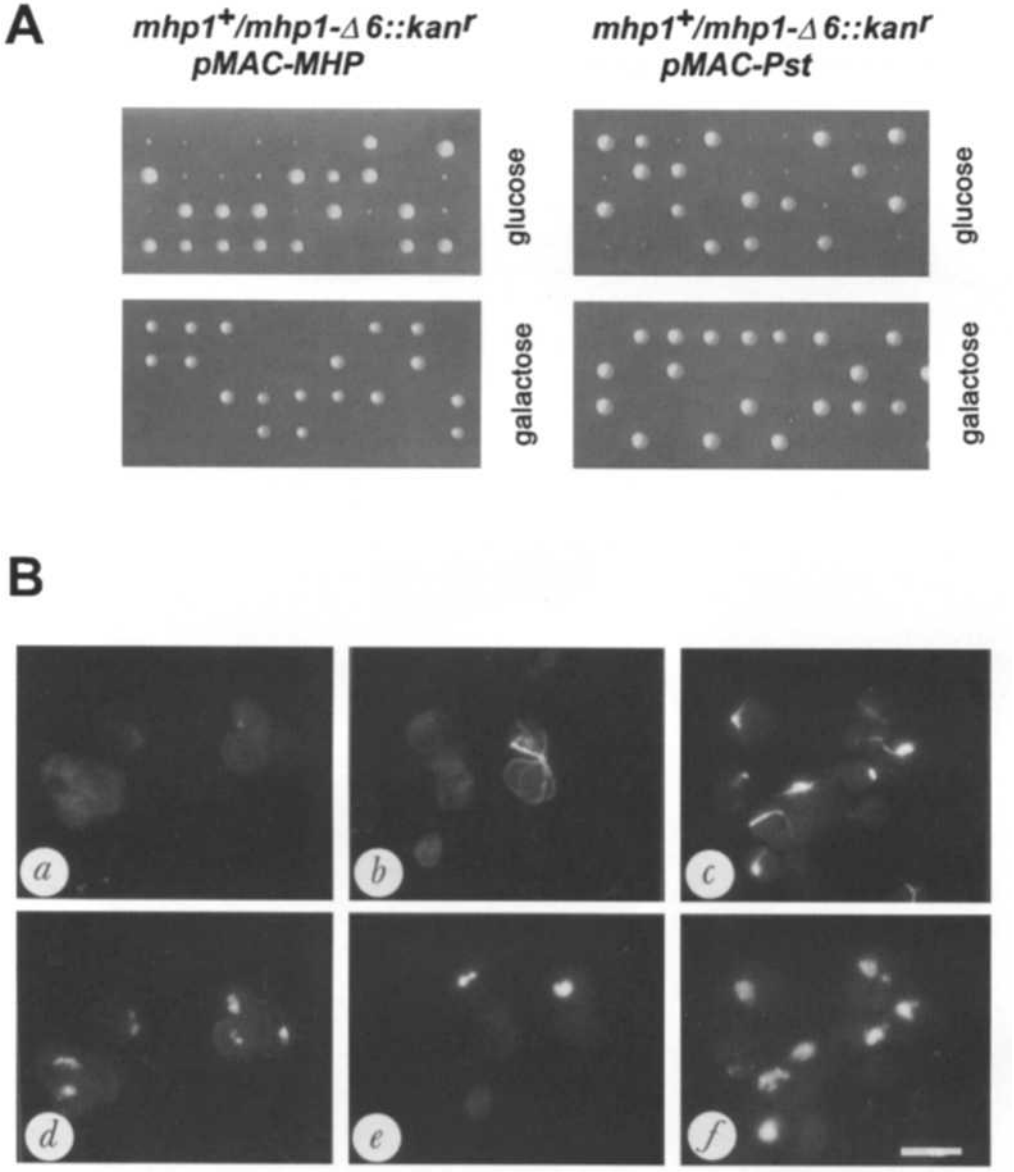

Figure 9. Compensation of *MHP1* null allele with *MHP1* and *mhp1-Δ3*. (*A*) Tetrad analysis of spores obtained from heterozygous *mhp1-Δ6* cells complemented with the full-length *MHP1* gene on plasmid pMAC-MHP or with the NH_2-terminal deletion allele *mhp1-Δ3* on the plasmid pMAC-Pst. Expression of the cloned regions on the centromeric plasmids MAC-MHP and pMAC-Pst is controlled by the GAL10 promoter. Dissections were carried out on plates containing glucose or galactose. (*B*) Analysis of MT phenotype in *MHP1* null mutant. Haploid *mhp1-Δ6* cells, rescued by the expression of *MHP1* from plasmid pMAC-MHP, grown in glucose for 10 h (*a* and *d*) or in galactose for 20 h (*b* and *e*), and the parental *mhp1+/mhp1-Δ6* cells carrying plasmid pMAC-MHP are shown (*c* and *f*). Anti-tubulin staining is shown in *a–c*, and DAPI staining is shown in *d–f*. Bar, 4.5 μm.

tion, no rescue was observed. To test possible effects of the pADNS plasmid, control experiments were also performed with the pADNS plasmid alone, but no rescue was observed. These results indicate that the partial rescue of the *mhp1-Δ1* and *mhp1-Δ6* mutations depends specifically on the expression of 205K MAP. From the Trp^+Leu^+ haploid cells, strain Y504 was generated and growth was analyzed under conditions that permitted or suppressed the expression of 205K MAP. After depriving the cells of glucose to silence the ADH promoter, no growth was observed for Y504 cells, while Y502 cells could grow with galactose instead of glucose as a carbon source, although initially at a slower rate (Fig. 10 *A*). We conclude that the viability of haploid *mhp1-Δ1* cells is partially restored by the expression of the 205K MAP, and that 205K MAP and Mhp1p share some functional similarity.

Analysis of MT structures in Y504 cells displayed an abnormal increase of cytoplasmic MTs in number and length. Y504 cells also showed an accumulation of cells with elongated (25%) and short spindles (15%). The elongated spindles contained thicker bundles of MTs than comparable wild-type cells, and the number and length of cytoplasmic MTs that emanate from the SPBs were increased. The axis of the mitotic spindle was altered in some cases, and multinucleated cells with multiple spindles could be observed (Fig. 10 *B*). In addition, the nuclear DNA staining appeared diffuse or fragmented and in some cases, no nuclear staining could be observed. Similar phenotypes were observed in haploid *mhp1-Δ6* cells, Y566, rescued with pADN-205. No such aberrant MT structures were observed in the diploid Y503 and Y565 cells, which suggests that the 205K MAP phenotype is recessive to the Mhp1p phenotype when both proteins are coexpressed, and that the phenotype observed in rescued cells is not only due to the expression of the exogenous 205K MAP, but also to the lack of a functional *MHP1*.

Discussion

MHP1 encodes a novel protein that has MT-binding activ-

Published December 1, 1996

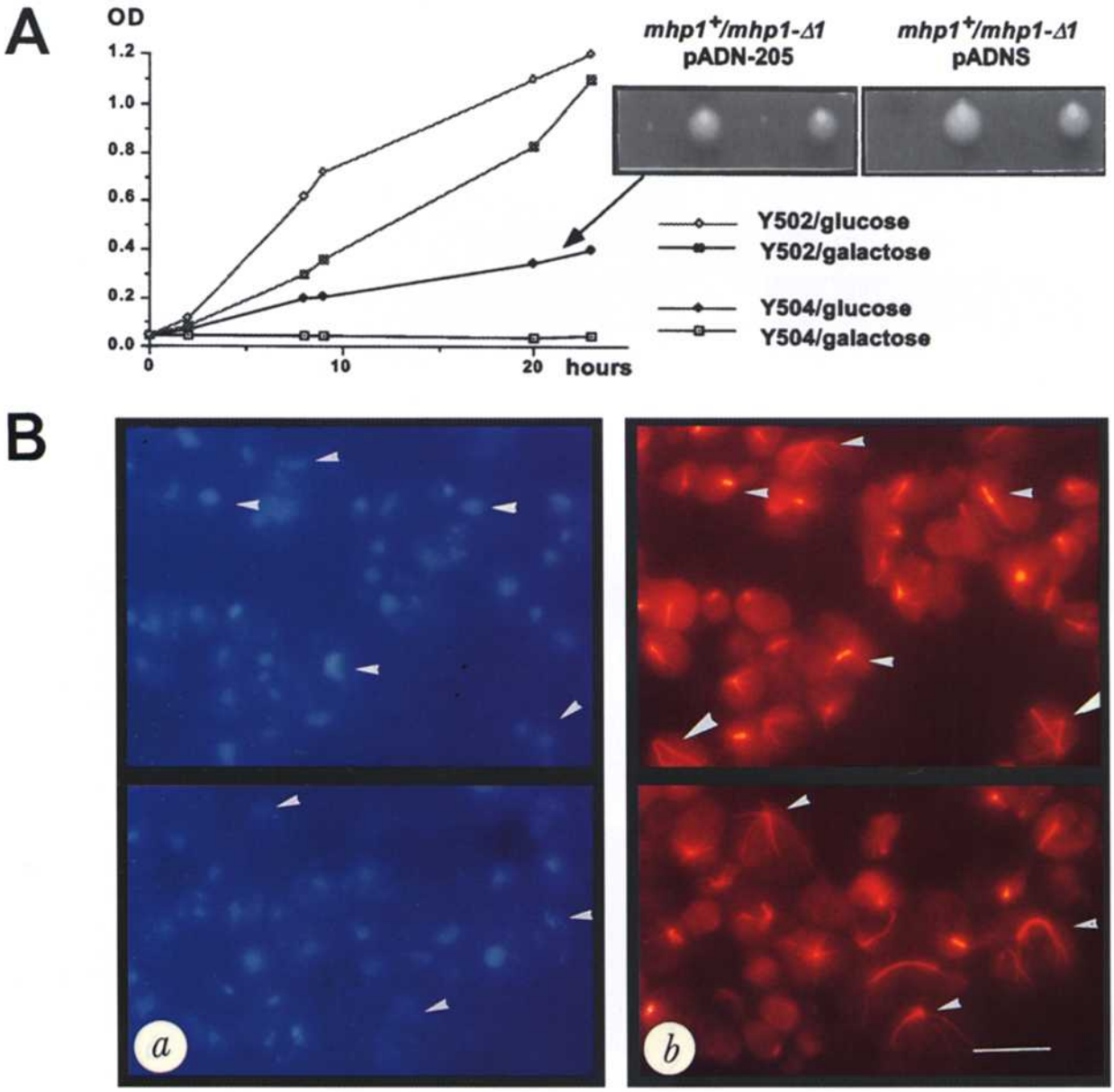

Figure 10. Partial rescue of the *mhp1-Δ1* mutation by the *Drosophila* 205K MAP. (*A*) Heterozygous Y503 and Y565 cells that carry the pADN-205 plasmid were dissected, and they gave rise to small colonies of rescued *mhp1-Δ1* or *mhp1-Δ6* haploid cells, termed Y504 and Y566, respectively. Growth curves of Y502 and rescued Y504 cells in glucose and galactose medium are shown, but they were similar for Y565 and Y566 cells. Cells were grown overnight and diluted to an OD_{600} of 0.05 so as to start with equivalent amounts of cells, and growth was monitored. No growth was observed for Y504 cells grown in galactose. (*Inset*) Typical tetrad of heterozygous *mhp1/mhp1-Δ1* cells transformed with the pADN-205 plasmid and of cells transformed with pADNS. (*B*) Analysis of MT structures in Y504 cells complemented with the *Drosophila* 205K MAP. DAPI staining is shown in *a*, and anti-tubulin staining is shown in *b*. Abnormally long and thick cytoplasmic MTs and mitotic MTs are indicated with small arrowheads, and multinucleated cells with multiple spindles are indicated with larger arrowheads. Bar, 4.5 μm.

ity in vitro. Its subcellular localization on MTs and the phenotype of aberrant MT structures in mutant cells suggest a function for Mhp1p in MT organization, particularly during mitosis. Mhp1p shares a short region of sequence homology with MAP2, MAP4, and tau, but not with 205K MAP. However, a polyclonal antibody directed against the *Drosophila* 205K MAP, which we used for expression cloning of *MHP1*, cross-reacts with Mhp1p. This antibody was previously shown to recognize mouse and human MAP 4 proteins (West, R.R., K.M. Tenbarge, M. Gorman, L.S.B. Goldstein, and J.B. Olmsted, 1988. *J. Cell Biol.* 107: 460a), but intriguingly, neither the mouse nor the human MAP4 species shares significant sequence homologies with the *Drosophila* 205K MAP. It is therefore likely that the anti-205K MAP antibody recognizes conserved MAP-specific epitopes, and that Mhp1p, 205K MAP, and MAP4 are structurally related proteins resulting from a homology that cannot be detected at the level of primary sequence comparison.

Mhp1p possesses structural features in common with

Published December 1, 1996

other known MAPs. Its estimated size on SDS gels is 50% larger than its calculated molecular weight, an observation made for other highly charged MAPs (Irminger-Finger et al., 1990; West et al., 1991). It is possible, however, that the 230-, 200-, and 150-kD proteins that are recognized by anti-MHP1 antibodies are isoforms of Mhp1p generated by posttranslational modification. Mhp1p is highly charged and the putative MT-binding domain is followed by an acidic COOH-terminal region, which is similar to the organization of tau and 205K MAP (Lee et al., 1988; Irminger-Finger et al., 1990). In contrast with MAP2, tau, and 205K MAP consisting of an acidic NH_2-terminal portion, a basic domain containing the MT-binding region, and in the case of tau and 205K MAP an acidic COOH-terminal region, Mhp1p contains alternating acidic and basic regions, and its acidity gradually increases from the NH_2-terminal to the COOH-terminal end. However, the density of potential phosphorylation sites gradually decreases from the NH_2-terminal to the COOH-terminal end (Fig. 1 *B*) and could lead to more negative charges within the NH_2-terminal half of the protein.

Phosphorylation has been characterized as an important mechanism for the regulation of the interaction of MAPs with MTs. In contrast to tau, MAP2, and 205K MAP, the potential kinase target sites on the amino acid sequence of Mhp1p localize within the NH_2-terminal two-thirds of the protein with fewer sites in the COOH-terminal portion containing the putative MT-binding region. It is therefore possible that MT binding in Mhp1p is less influenced by phosphorylation than by other functions residing in the NH_2-terminal portion of Mhp1p. An important function for the NH_2-terminal domain of Mhp1p is also suggested by the phenotype induced by the *mhp1-Δ3* allele (Fig. 9).

We have demonstrated that the region of Mhp1p sufficient and essential for MT binding is located within the COOH-terminal 210 amino acid residues of Mhp1p. The localization of the AP homologous sequence motif within this region is consistent with its role in MT binding. However, the region found to be homologous to the AP motif is less basic than other AP sequences, although flanked by sequences containing basic residues (Figs. 1 *B* and 2). It is conceivable that these adjacent basic sequences participate in MT binding in Mhp1p or that the binding is achieved without a predominantly basic charge, as was reported for binding motifs of other MAPs (Hemphill et al., 1992). In support of this idea is the finding that an interrepeat region of the AP repeats in tau has higher MT affinity than a single repeat (Goode and Feinstein, 1994). A significant contribution of the sequences outside the AP motif, which was also reported for MAP4 (Olson et al., 1995), might explain why for Mhp1p a single repeat could be sufficient for MT binding. The reduced binding activity of the deletion N1300, containing the AP-homologous sequence but not the entire COOH terminus of Mhp1p, could be due to a participation of sequences close to the COOH terminus to MT binding. It is also possible that the protein folding of the deletion N1300 is altered when the COOH terminus is missing.

The generation of Mhp1p-specific antibodies permitted the identification of Mhp1p as a 200-kD protein on Western blots comigrating with bacterially produced Mhp1p. Minor bands of 150, 90, and 60 kD also react with anti-MHP1 and are increased in Y509 cells overproducing Mhp1p. These proteins could be degradation products, isoforms, or products of differential transcription and translation. The former possibility would be consistent with the expression of a 2.8-kb mRNA observed in wild-type cells, which hybridized to the 3′-end probe of *MHP1* (Fig. 7 *A*). The differential transcription and/or translation could be a regulatory mechanism for the expression of *MHP1* gene products encoding different functions. The localization of the anti-MHP1–reactive epitope to cytoplasmic and nuclear MTs is consistent with MT-binding experiments. However, since anti-MHP1 was generated against the COOH-terminal peptide C1188p, we cannot exclude that the staining observed in immunofluorescence analyses is due to cross-reaction with isoforms of Mhp1p <200 kD, as observed on Western blots.

Indirect evidence that differential transcription and translation could lead to functional products comes from the viable *mhp1-Δ2* mutation, derived from an insertion in the NH_2-terminal half of the protein-coding region, that disrupts the ORF after residue 557. It seems likely that *mhp1-Δ2* mutant cells express both NH_2- and COOH-terminal truncation products of *MHP1*, since two separate transcripts are detected. The translation of a COOH-terminal 90-kD protein, detected with anti-MHP antibodies in *mhp1-Δ2* cells (Fig. 7 *B*), could be initiated at one of the candidate methionine initiation codons located at positions 598 and 612 (Fig. 2 *A*). The *mhp1-Δ4* mutation deleting coding sequences from residues 1–613, including the two potential translation initiation codons, is lethal in haploid cells. Also, the *mhp1-Δ5* mutation, deleting residues downstream of the *URA3*$^+$ insertion site in the *mhp1-Δ2* mutation, results in lethality in haploid cells, supporting the conclusion that transcription initiation can occur at positions 598 or 612. Viability of the null mutant could also be restored with plasmid pMAC-Pst (Fig. 9 *A*) containing the region downstream from amino acid position 561, demonstrating that the COOH-terminal region is sufficient for viability without the NH_2-terminal portion of the gene expressed separately.

The results of gene disruption experiments and in vitro MT-binding experiments suggest that Mhp1p is organized in a COOH-terminal domain (residues 821–1,398) essential for MT binding, and an NH_2-terminal domain (residues 1–561) important for proper function of Mhp1p, which is absent in the *mhp1-Δ3* mutation. Deleting the region of *MHP1* that includes the domain essential for MT binding leads to lethality in haploid cells (Fig. 6), but the NH_2-terminal deletion allele *mhp1-Δ3* can partially compensate lethality of the complete null allele, demonstrating that *mhp1-Δ3* provides sufficient *MHP1* function for viability (Fig. 9). The overexpression of the *mhp1-Δ3* allele leads to reduced growth with a specific phenotype of heterogeneously arrested cells at different stages of mitosis mostly before the onset of anaphase. The number of mutant cells is correlated with the expression level of the mutant protein. In contrast with mutants effecting SPB duplication, such as *kar1* and *cdc31* (Vallen et al., 1994), *mhp1-Δ3* cells arrest at various times of spindle formation, and it is the number of cells with elongated spindles and divided nuclei that becomes more reduced when the expression of *mhp1-Δ3* is increased (Table III). The hetero-

geneous phenotype of inhibition of the progression through anaphase strongly suggests a structural defect compatible with a role in MT stabilization and/or formation.

A different phenotype was observed with the overexpression of the entire *MHP1*. The additional production of Mhp1p results in increased formation and/or stabilization of cytoplasmic MTs. It is possible that the protein encoded on *mhp1-Δ3* is missing a signal that retains it in the cytoplasm or that the truncated form is more efficiently transported to the nucleus interacting with nuclear MTs. Reports from a number of laboratories demonstrate that the interaction of MAP4-type proteins with MTs is regulated during the cell cycle by phosphorylation by specific kinases (Aizawa et al., 1991; Vandré et al., 1991; Ookata et al., 1995). Therefore, a possible explanation for the cell cycle block observed in *mhp1-Δ3* cells and the phenotype induced by overexpression of *MHP1* could be deregulated phosphorylation. Increased levels of Mhp1p or the mutant protein encoded on *mhp1-Δ3* could expend the capacities of different specific kinases that regulate the interaction of Mhp1p with MTs. Mutational analyses and biochemical approaches should provide information on the function of the NH_2-terminal domain of Mhp1p and help to identify regulatory factors that interact with Mhp1p, such as kinases.

All mutations induced by gene disruption, overexpression of the entire *MHP1*, or the COOH-terminal part of *MHP1* affect the formation of MTs and the function of MTs during the progression through cell cycle. A reduced gene dosage in heterozygous *mhp1⁺/mhp1-Δ1::TRP1* and *mhp1⁺/mhp1-Δ1::kan^r* cells appears to affect cells at late mitosis, since in an exponentially growing culture, the number of cells at this stage is elevated. In cells overexpressing the entire *MHP1* gene, we observe long cytoplasmic MTs, indicating that an increased concentration of Mhp1p promotes MT polymerization and/or increases MT stability. In complete null mutants Y564, expressing minimal amounts of Mhp1p from the "silenced" GAL10 promoter, the formation of MTs is reduced. In Y504 and Y566 cells rescued by the expression of 205K MAP, an excess of aberrant MT structures can be observed as a result of the MT-stabilizing effect of overexpressed 205K MAP. A similar phenotype had been observed in the fission yeast when mammalian MAP4 was overexpressed (Olmsted, J.B., and J.R. McIntosh. 1994. *Mol. Biol. Cell.* 5:169a). These data suggest that Mhp1p regulates the fine tuning of MT stability that cannot be achieved by the expression of a truncated form of Mhp1p or by a surrogate MAP from another species. Future research will focus on the timing and nature of the essential interactions of Mhp1p with MTs by using *mhp1-Δ6* haploid cells complemented by mutagenized inducible *MHP1* on expression plasmids. Overall, the system described here should also permit the determination of functions generally possessed by MAPs by domain-swapping experiments between Mhp1p and other MAPs, and by the testing of hybrid proteins in *MHP1* null mutants.

We are grateful to Drs. A. Pereira, R. Ortega Perez, and W.D. Heyer for helpful comments and critical reading of the manuscript; M. Princevalle for generation of anti-MHP1 antibodies; and N. Mathis for excellent technical help. We are indebted to Dr. L. Huber for useful suggestions and discussions, Dr. O. Schaad for specific computer programs, and Prof. J. Olmsted for the mouse MAP4 cDNA clone.

This work was supported by a grant from the Swiss National Science Foundation (to S.J. Edelstein).

Received for publication 1 July 1996 and in revised form 9 August 1996.

References

Aizawa, H., H. Kawasaki, H. Murofushi, S. Kotani, K. Suzuki, and H. Sakai. 1989. A common amino acid sequence in 190-kDa microtubule-associated protein and tau for the promotion of microtubule assembly. *J. Biol. Chem.* 264:5885–5890.

Aizawa, H., Y. Emori, H. Murofushi, H. Kawasaki, H. Sakai, and K. Suzuki. 1990. Molecular cloning of a ubiquitously distributed microtubule-associated protein with M_r 190,000. *J. Biol. Chem.* 265:13849–13855.

Aizawa, H., M. Kamijo, Y. Ohba, A. Mori, K. Okuhara, H. Kawasaki, H. Murofushi, K. Suzuki, and H. Yasuda. 1991. Microtubule destabilization by cdcd2/H1 histone kinase: phosphorylation of a "Pro-rich region" in the microtubule-binding domain of MAP4. *Biochem. Biophys. Res. Commun.* 179:1620–1626.

Barnes, G., A. Louie, and D. Botstein. 1992. Yeast proteins associated with microtubules *in vitro* and *in vivo*. *Mol. Biol. Cell.* 3:29–47.

Bellocq, C., I. Andrey-Tornare, A.-M. Paunier, B. Maeder, L. Paturle, D. Job, J. Haiech, and S. Edelstein. 1992. Purification of assembly-competent tubulin from *Saccharomyces cerevisiae*. *Eur. J. Biochem.* 210:343–349.

Berlin, V., C.A. Styles, and G.R. Fink. 1990. BIK1, a protein required for microtubule function during mating and mitosis in *Saccharomyces cerevisiae*, colocalizes with tubulin. *J. Cell Biol.* 111:2573–2586.

Botstein, D., S.C. Falco, S.E. Stewart, M. Brennan, S. Scherer, D.T. Stinchcomb, K. Struhl, and R.W. Davis. 1979. Sterile host yeasts (SHY): a eukaryotic system of biological containment for recombinant DNA experiments. *Gene (Amst.).* 8:17–24.

Bulinski, J.C., and G.G. Borisy. 1979. Self-assembly of microtubules in extracts of cultured HeLa cells and the identification of HeLa microtubule-associated protein. *Proc. Natl. Acad. Sci. USA.* 76:293–297.

Bulinski, J.C., and G.G. Borisy. 1980. Widespread distribution of a 210,000 mol wt microtubule-associated protein in cells and tissues of primates. *J. Cell Biol.* 87:802–808.

Chapin, S.J., and J.C. Bulinski. 1991. Non-neural 210 × 10^3 M_r microtubule-associated protein (MAP4) contains a domain homologous to the microtubule-binding domains of neural MAP2 and tau. *J. Cell Sci.* 98:27–36.

Chou, P., and G.D. Fasman. 1978. Prediction of the secondary structure of proteins from their amino acid sequence. *Adv. Enzymol.* 47:45–147.

Cleveland, D.W., S.Y. Hwo, and M.W. Kirschner. 1977. Physical and chemical properties of purified tau factor and the role of tau in microtubule assembly. *J. Mol. Biol.* 116:227–247.

Colicelli, J., C. Birchmeier, T. Michaeli, K. O'Neill, M. Riggs, and M. Wigler. 1989. Isolation and characterization of a mammalian gene encoding a high-affinity cAMP phosphodiesterase. *Proc. Natl. Acad. Sci. USA.* 86:3599–3603.

Devereux, J., P. Haeberli, and O. Smithies. 1984. A comprehensive set of sequence analysis programs for the VAX. *Nucleic Acids Res.* 12:387–395.

Diaz-Nido, J., L. Serrano, E. Mendez, and J. Avila. 1988. A casein kinase II-related activity is involved in phosphorylation of microtubule-associated protein MAP1B during neuroblastoma cell differentiation. *J. Cell Biol.* 106:2057–2065.

Edelmann, A.M., D.K. Blumenthal, and E.G. Krebs. 1987. Protein serine/threonine kinases. *Annu. Rev. Biochem.* 56:567–613.

Garnier, J., D.J. Osguthorpe, and B. Robson. 1978. Analysis of the accuracy and implications of simple methods for predicting the secondary structure of globular proteins. *J. Mol. Biol.* 120:97–120.

Goldstein, L.S.B., R.A. Laymon, and J.R. McIntosh. 1986. A microtubule-associated protein in *Drosophila melanogaster*: identification, characterization, and isolation of coding sequences. *J. Cell Biol.* 107:2076–2087.

Gonzales, G.A., K.K. Yamamoto, W.H. Fischer, D. Karr, P. Menzel, I. Biggs, W.W. Vale, and M.R. Montminy. 1989. A cluster of phosphorylation sites on the cyclic AMP-regulated nuclear factor CRBE predicted by its sequence. *Nature (Lond.).* 337:749–752.

Goode, B.L., and S.C. Feinstein. 1994. Identification of a novel microtubule binding and assembly domain in the developmentally regulated inter-repeat region of tau. *J. Cell Biol.* 124:769–782.

Hasek, J., J. Jochova, P. Draber, V. Viklicky, and E. Streiblova. 1991. Localization of a 210-kD microtubule-interacting protein in the yeast *Saccharomyces cerevisiae*. *Can. J. Microbiol.* 38:149–152.

Hemphill, A., M. Affolter, and T. Seebeck. 1992. A novel microtubule-binding motif identified in a high molecular weight microtubule-associated protein from *Trypanosoma brucei*. *J. Cell Biol.* 117:95–103.

Hoyt, M.A., T. Sterns, and D. Botstein. 1990. Chromosome instability mutants of *Saccharomyces cerevisiae* that are defective in microtubule-mediated processes. *Mol. Cell. Biol.* 10:223–234.

Hoyt, A.M., L. He, K.K. Loo, and W.S. Saunders. 1992. Two *Saccharomyces cerevisiae* kinesin-related gene products required for mitotic spindle assembly. *J. Cell Biol.* 118:109–120.

Hurt, E.C. 1988. A novel nucleoskeletal-like protein located at the nuclear periphery is required for the life cycle of the yeast *Saccharomyces cerevisiae*. *EMBO (Eur. Mol. Biol. Organ.) J.* 7:4323–4334.

Hyman, A.A., K. Middleton, M. Centola, T.J. Mitchison, and J. Carbon. 1992. Microtubule-motor activity of a yeast centromere-binding protein complex. *Nature (Lond.).* 359:533–539.

Interthal, H., C. Bellocq, J. Bahler, V.I. Bashkirov, S. Edelstein, and W.D. Heyer. 1995. A role of Sep1 (=Kem1, Xrn1) as a microtubule-associated protein in *Saccharomyces cerevisiae*. *EMBO (Eur. Mol. Biol. Organ.) J.* 14: 1057–1066.

Irminger-Finger, I., R.A. Laymon, and L.S.B. Goldstein. 1990. Analysis of the primary sequence and microtubule-binding region of the *Drosophila* 205K MAP. *J. Cell Biol.* 111:2563–2572.

Izant, J., J. Weatherbee, and J.R. McIntosh. 1983. A microtubule-associated protein antigen unique to mitotic spindle microtubules in PtK1 cells. *J. Cell Biol.* 96:424–434.

Jiang, W., K. Middleton, H. Yoon, C. Fouquet, and J. Carbon. 1993. An essential yeast protein, CBF5p, binds *in vitro* to centromeres and microtubules. *Mol. Cell. Biol.* 13:4884–4893.

Kilmartin, J.V., and A.E. Adams. 1984. Structural rearrangements of tubulin and actin during the cell cycle of the yeast *Saccharomyces*. *J. Cell Biol.* 98: 922–933.

Kilmartin, J.V., B. Wright, and C. Milstein. 1982. Rat monoclonal anti-tubulin antibodies derived by using a new nonsecreting rat cell line. *J. Cell Biol.* 93: 576–582.

Kilmartin, J.V., S.L. Dyos, D. Kershaw, and J.T. Finch. 1993. A spacer protein in the *Saccharomyces cerevisiae* spindle pole body whose transcript is cell cycle-regulated. *J. Cell Biol.* 123:1175–1184.

Kimble, M., A.L. Khodjakov, and R. Kuriyama. 1992. Identification of ubiquitous high-molecular-mass, heat-stable microtubule-associated proteins (MAPs) that are related to the *Drosophila* 205-kDa MAP but are not related to the mammalian MAP4. *Proc. Natl. Acad. Sci. USA.* 89:7693–7697.

Lee, G. 1993. Non-motor microtubule-associated proteins. *Curr. Opin. Cell Biol.* 5:88–94.

Lee, G., N. Cowan, and M. Kirschner. 1988. The primary structure and heterogeneity of tau protein from mouse brain. *Science (Wash. DC).* 239:265–288.

Lewis, S.A., D. Wang, and N.J. Cowan. 1988. Microtubule-associated protein MAP2 shares a microtubule-binding motif with tau protein. *Science (Wash. DC).* 242:936–939.

Li, Y.-Y., E. Yeh, and K. Bloom. 1993. Disruption of mitotic spindle orientation in a yeast dynein mutant. *Proc. Natl. Acad. Sci. USA.* 90:10096–10100.

Lillie, S.H., and S.S. Brown. 1992. Suppression of a myosin defect by a kinesin-related gene. *Nature (Lond.).* 356:358–361.

Maniatis, T., E.F. Fritsch, and J. Sambrook. 1989. Molecular Cloning: a Laboratory Manual. Cold Spring Harbor Laboratory Press, Cold Spring Harbor, NY. 545 pp.

McMillan, J.N., and K. Tatchell. 1994. The *JNM1* gene in the yeast *Saccharomyces cerevisiae* is required for nuclear migration and spindle orientation during the mitotic cell cycle. *J. Cell Biol.* 125:143–158.

Meluh, P.B., and M.D. Rose. 1990. *KAR3*, a kinesin-related gene required for yeast nuclear fusion. *Cell.* 60:1029–1041.

Munro, S., and H.R.B. Pelham. 1984. Use of peptide tagging to detect proteins expressed from cloned genes: deletion mapping functional domains of *Drosophila* hsp70. *EMBO (Eur. Mol. Biol. Organ.) J.* 3:3087–3093.

Murphy, D.B., R.B. Vallee, and G.G. Borisy. 1977. Identity and polymerization-stimulatory activity of the non-tubulin proteins associated with microtubules. *Biochemistry.* 16:2598–2605.

Noble, M., S.A. Lewis, and N.J. Cowan. 1989. The microtubule-binding domain of microtubule-associated protein MAP1B contains a repeated sequence motif unrelated to that of MAP2 and tau. *J. Cell Biol.* 109:3367–3376.

Olmsted, J.B. 1986. Analysis of cytoskeletal structures using blot-purified monospecific antibodies. *Methods Enzymol.* 134:467–472.

Olson, K.R., J.R. McIntosh, and J.B. Olmsted. 1995. Analysis of MAP4 function in living cells using green fluorescent protein (GFP) chimeras. *J. Cell Biol.* 130:639–650.

Ookata, K., S. Hisanaga, J.C. Bulinski, H. Murofushi, H. Aizawa, T.J. Itoh, H. Hotani, E. Okumura, K. Tachibana, and T. Kishimoto. 1995. Cyclin B interaction with microtubule-associated protein 4 (MAP4) targets p34cdc2 kinase to microtubules and is a potential regulator of M-phase microtubule dynamics. *J. Cell Biol.* 128:849–862.

Ortega Perez, R., I. Irminger-Finger, J.F. Arrighi, N. Capelli, D. van Tuinen, and G. Turian. 1994. Identification and partial purification of calmodulin-binding microtubule-associated proteins from *Neurospora crassa*. *Eur. J. Biochem.* 226:303–310.

Pasqualone, D., and T.C. Huffaker. 1994. *STU1*, a suppressor of a β-tubulin mutation, encodes a novel and essential component of the yeast mitotic spindle. *J. Cell Biol.* 127:1973–1984.

Pearson, R.B., J.R. Woodgett, P. Cohen, and B.E. Kemp. 1985. Substrate specificity of a multifunctional calmodulin-dependent protein kinase. *J. Biol. Chem.* 260:14471–14476.

Pearson, W.R., and D.J. Lipman. 1988. Improved tools for biological sequence comparison. *Proc. Natl. Acad. Sci. USA.* 85:2444–2448.

Pereira, A., J. Doshen, E. Tanaka, and L.S.B. Goldstein. 1992. Genetic analysis of a *Drosophila* microtubule-associated protein. *J. Cell Biol.* 116:377–383.

Roberts, B. 1989. Nuclear location signal-mediated protein transport. *Biochem. Biophys. Acta.* 1008:263–280.

Roof, D.M., P.M. Meluh, and M.D. Rose. 1992. Kinesin-related proteins required for assembly of the mitotic spindle. *J. Cell Biol.* 118:95–108.

Rose, M.D., F. Winston, and P. Hierter. 1990. Methods in Yeast Genetics. A Laboratory Course Manual. Cold Spring Harbor Laboratory Press, Cold Spring Harbor, NY. 198 pp.

Rothstein, R.J. 1983. One step gene disruption in yeast. *Methods Enzymol.* 101: 202–210.

Sanger, F., S. Michlen, and A.R. Coulson. 1977. DNA sequencing with chain terminating inhibitors. *Proc. Natl. Acad. Sci. USA.* 74:5463–5467.

Schoenfeld, T.A., L. McKerracher, R. Obar, and R.B. Vallee. 1989. MAP 1A and MAP 1B are structurally related microtubule-associated proteins with distinct developmental patterns in the CNS. *J. Neurosci.* 9:1712–1730.

Sherman, F., G.R. Fink, and J.B. Hicks. 1986. Methods in Yeast Genetics. Cold Spring Harbor Laboratory, Cold Spring Harbor, NY. 163–167.

Sikorski, R.S., and P. Hieter. 1989. A system of shuttle vectors and yeast host strains designed for efficient manipulation of DNA in *Saccharomyces cerevisiae*. *Genetics.* 122:19–27.

Stearns, T., A. Hoyt, and D. Botstein. 1990. Yeast mutants sensitive to antimicrotubule drugs define three genes that regulate microtubule function. *Genetics.* 124:251–262.

Strohm, M., P. Vollmer, T.J. Tan, and D. Gallwitz. 1993. A yeast GTPase-activating protein that interacts specifically with a member of the YPT/RAB family. *Nature (Lond.).* 361:736–739.

Studier, W., A.H. Rosenberg, J.J. Dunn, and J.W. Dubendorff. 1990. Use of the T7 RNA polymerase to direct expression of cloned genes. *Methods Enzymol.* 185:60–89.

Vallee, R.B. 1982. A taxol-dependent procedure for the isolation of microtubules and microtubule-associated proteins (MAPs). *J. Cell Biol.* 92:435–442.

Vallen, E.A., W. Ho, M. Winey, and M.D. Rose. 1994. Genetic interactions between CDC31 and KAR1, two genes required for duplication of the microtubule organizing center in *Saccharomyces cerevisiae*. *Genetics.* 137:407–422.

Vandré, D.D., V.E. Centonze, J. Peloquin, R.M. Tombes, and G.G. Borisy. 1991. Proteins of the mammalian mitotic spindle: phosphorylation/dephosphorylation of MAP-4 during mitosis. *J. Cell Sci.* 98:577–588.

Wach, A., A. Brachat, R. Pöhlmann, and P. Philippsen. 1994. New heterologous modules for classical or PCR-based gene disruptions in *Saccharomyces cerevisiae*. *Yeast.* 10:1793–1808.

West, R.R., K.M. Tenbarge, and J.B. Olmsted. 1991. A model for microtubule-associated protein 4 structure. *J. Biol. Chem.* 266:21886–21896.

Wiche, G., C. Oberkanins, and A. Himmler. 1991. Molecular structure and function of microtubule-associated proteins. *Int. Rev. Cytol.* 124:217–273.